# NATIONAL ADVISORY COMMITTEE FOR AERONAUTICS

TECHNICAL NOTE

No. 1769

## THE FLEXIBLE RECTANGULAR WING IN ROLL AT SUPERSONIC FLIGHT SPEEDS

By Warren A. Tucker and Robert L. Nelson

Langley Aeronautical Laboratory
Langley Field, Va.


Washington
December 1948

NATIONAL ADVISORY COMMITTEE FOR AERONAUTICS

TECHNICAL NOTE NO. 1769



# THE FLEXIBLE RECTANGULAR WING IN ROLL AT SUPERSONIC FLIGHT SPEEDS

By Warren A. Tucker and Robert L. Nelson

## SUMMARY

The problem of the loss in rolling effectiveness at supersonic flight speeds is considered for the case of the rectangular wing. Equations are obtained from which can be calculated either the loss in rate of roll due to flexibility or the torsional stiffness required to maintain a given rate of roll, for two assumed variations of the spanwise distribution of torsional stiffness.

A computation form and figures are provided so that calculations can be made without reference to the details of the analysis.

## INTRODUCTION

The problem of the flexible rolling wing in subsonic flow has been dwelt upon by many investigators, who have devised numerous methods of solution. References 1 and 2 were found valuable in the preparation of the present paper; reference 1 notes several other useful papers. So far as the domain of supersonic speeds is concerned, however, little work has been done on the problem.

The fundamental relations between the aerodynamic and the elastic forces are, of course, valid for any flight speed. The aerodynamic forces themselves, however, are critically dependent on the flight speed because of the vast difference in flow behavior between the subsonic and the supersonic regions. Any solution of the aeroelastic problem at supersonic speeds, then, must consider aerodynamic forces calculated by the various methods peculiar to the supersonic zone.

As a first step toward a solution of the problem, a treatment is given of the relatively simple case of loss in rolling effectiveness of the rectangular wing with constant-chord ailerons extending inboard from the wing tips. (See fig. 1.) The methods used are in general based on the linearized equations for supersonic flow. Due consideration is given to three-dimensional effects. The torsional stiffness of the wing is assumed to vary either linearly with the distance outboard from the wing center line or as the cube of this distance.

Because of the relative complexity of the equations involved in the analysis, a computation form and figures are provided from which calculations can be made without reference to the details of the analysis.

## SYMBOLS

| | |
|---|---|
| $A$ | aspect ratio $(b/c$ or $b^2/S)$ |
| $b$ | wing span |
| $b_a$ | total aileron span |
| $c$ | wing chord |
| $c_a$ | aileron chord |
| $S$ | wing area $(bc)$ |
| $s$ | semispan $(b/2)$ |
| $y$ | distance out from wing center line (see fig. 1) |
| $M$ | free-stream Mach number |
| $\beta = \sqrt{M^2 - 1}$ | |
| $\gamma$ | ratio of specific heat at constant pressure to specific heat at constant volume (1.40 for air) |
| $p_o$ | free-stream static pressure |
| $q$ | free-stream dynamic pressure $\left(\frac{\gamma}{2} p_o M^2\right)$ |
| $P$ | lifting pressure |
| $C_p$ | lifting-pressure coefficient $(P/q)$ |
| $C_{p_\infty}$ | additional two-dimensional lifting-pressure coefficient due to aileron deflection $(4\delta/\beta)$ |
| $\delta$ | deflection of one aileron |
| $\theta$ | angle of twist at any spanwise station |
| $\theta_r$ | angle of twist at reference station (midspan of aileron) |
| $pb/2V$ | wing-tip helix angle |

| | |
|---|---|
| $p$ | rolling angular velocity |
| $V$ | free-stream velocity |
| $l$ | rolling moment |
| $C_l$ | rolling-moment coefficient $(l/qSb)$ |
| $C_{l_\delta}$ | rolling-moment-effectiveness coefficient for two ailerons $\left(\frac{\partial C_l}{\partial \delta}\right)$ |
| $C_{l_p}$ | damping-in-roll coefficient $\left(\frac{\partial C_l}{\partial \frac{pb}{2V}}\right)$ |
| $C_{l_{\theta_r}}$ | rolling-moment-loss coefficient $\left(\frac{\partial C_l}{\partial \theta_r}\right)$ |
| $T$ | torque at any spanwise station $\left(\int_y^s m\, dy\right)$ |
| $m$ | pitching moment about midchord at any spanwise station |
| $GJ$ | torsional-stiffness parameter $\left(\frac{T}{d\theta/dy}\right)$ |
| $m_\theta$ | torsional-stiffness parameter $(T/\theta)$ |
| $m_{\theta_r}$ | torsional-stiffness parameter at reference station (midspan of aileron) |
| $k$ | constant of proportionality for stiffness distribution |
| $w_1, w_2$ | constants of proportionality for twist distribution |
| $F$ | trailing-edge angle reduction factor |
| $\phi$ | disturbance-velocity potential |
| $x, y$ | Cartesian coordinates parallel and normal, respectively, to free-stream direction (see fig. 13(a)), for field points |
| $\xi, \eta$ | Cartesian coordinates parallel and normal, respectively, to free-stream direction (see fig. 13(a)), for source points |

$$B \equiv \frac{\beta A}{4} \frac{b_a}{b} \frac{c_a}{c} \left(1 - \frac{c_a}{c}\right) - \frac{1}{24} \left(\frac{c_a}{c}\right)^2 \left(3 - 2 \frac{c_a}{c}\right)$$

$$R_1 \equiv 2 \frac{b_a}{b} - \frac{5}{4} \left(\frac{b_a}{b}\right)^2$$

$$R_2 \equiv 4 \frac{b_a}{b} - \frac{15}{2} \left(\frac{b_a}{b}\right)^2 + 5 \left(\frac{b_a}{b}\right)^3 - \frac{19}{16} \left(\frac{b_a}{b}\right)^4$$

Subscripts:

| | |
|---|---|
| R | rigid |
| 0 | sea level |
| 1,2,3 | used with $\phi$ and $C_p$ to indicate various regions of wing |

All angles are in radians, unless otherwise specified.

## ANALYSIS

In a steady roll, the resultant rolling moment acting on the wing is zero. This statement can be written in equation form as

$$\beta C_{l_\delta} \delta - \left(-\beta C_{l_p}\right) \frac{pb}{2V} - \beta C_{l_{\theta_r}} \theta_r = 0 \qquad (1)$$

where $\beta C_{l_\delta}$ is the rolling-moment-effectiveness coefficient of the ailerons, $\beta C_{l_p}$ is the damping-in-roll coefficient, and $\beta C_{l_{\theta_r}}$ is the rolling-moment-loss coefficient resulting from the flexibility of the wing. The quantity $\beta$ is retained merely for convenience in the subsequent analysis. The positive sign is given to the quantities $\beta C_{l_\delta}$, $-\beta C_{l_p}$, and $\beta C_{l_{\theta_r}}$.

The following equations can be written from equation (1):

$$\frac{pb/2V}{\delta} = \frac{\beta C_{l_\delta} - \beta C_{l_{\theta_r}} \frac{\theta_r}{\delta}}{-\beta C_{l_p}} \qquad (2)$$

$$\frac{pb/2V}{(pb/2V)_R} = 1 - \frac{\beta C_{l_{\theta_r}}}{\beta C_{l_\delta}} \frac{\theta_r}{\delta} \tag{3}$$

Equations (1) to (3) are applicable to flight at either subsonic or supersonic speeds. The problem, then, is simply to determine the values of the various quantities at supersonic speeds. For a given wing-aileron configuration, equations for $\beta C_{l_\delta}$ and $-\beta C_{l_p}$ can be found from references 3 and 4, respectively. The remainder of the analysis is devoted to the derivation of expressions for the rolling-moment-loss coefficient $\beta C_{l_{\theta_r}}$ and the twist parameter $\theta_r/\delta$. Those readers who are more interested in the application than in the derivation are advised to turn to the section entitled "Computation Procedure and Discussion."

Torque.- A knowledge of the spanwise distribution of twist $\theta$ is necessary for the determination of either $\beta C_{l_{\theta_r}}$ or $\theta_r/\delta$. The twist at any section is found from considerations of the aerodynamic torque and the elastic forces acting on the wing. The aerodynamic torque is assumed to result solely from the moment about the wing midchord line of the pressure resulting from aileron deflection. This assumption implies that the centers of pressure of the lift forces resulting from rolling and from twist are so near the elastic axis as to contribute only a negligibly small twisting moment. Because the elastic axis of a rectangular wing designed for supersonic speeds would be expected to lie near the midchord line (much as in the case of a subsonic wing, where the elastic axis and the line of aerodynamic centers are not too far separated) and because the centers of pressure of the forces resulting from rolling and from twist are near the midchord line, the assumption appears reasonable. In addition, the loads caused by aileron deflection are assumed to be independent of wing twist, and the aileron itself is assumed not to twist. An important result of making these assumptions is the elimination of any necessity for using a successive approximation method.

The aerodynamic torque T at any spanwise station y is simply the total moment acting outboard of the station. That is,

$$T = \int_y^s m \, dy \tag{4}$$

where m is the pitching moment about the midchord at any station and is assumed to result solely from the pressures caused by aileron deflection. These pressures were taken from the equations given in figure 2(a) of reference 3. The resulting equations for the torque were

very cumbersome; therefore, the exact expression was approximated by two simple expressions, one representing a constant torque over the part of the span inboard of the aileron (the value of this torque was taken equal to the greatest value given by the exact expression) and the other representing a torque decreasing linearly along the aileron span to zero at the wing tip. The approximate equation for the torque per unit aileron deflection inboard of the aileron is

$$\frac{T}{C_{p_\infty} q c^3} = \frac{B}{\beta} \tag{5a}$$

where $0 \leqq \frac{y}{s} \leqq 1 - \frac{b_a}{b}$ and the approximate equation for the torque over the aileron span is

$$\frac{T}{C_{p_\infty} q c^3} = \frac{B}{\beta} \frac{b}{b_a} \left(1 - \frac{y}{s}\right) \tag{5b}$$

where $1 - \frac{b_a}{b} \leqq \frac{y}{s} \leqq 1$. A comparison of the torque distribution obtained from the exact and approximate equations is shown in figure 2 for a particular configuration and for two values of $\beta$. The same degree of approximation can be expected for other configurations. The principal factor governing the closeness of approximation is the value of $\beta$; as $\beta$ increases, the approximation approaches more closely the exact variation.

Twist.- The twist $\theta$ at any spanwise station $y$ can be expressed as

$$\theta = \int_0^y \frac{d\theta}{dy} \, dy \tag{6}$$

therefore, if an expression can be found for $d\theta/dy$, the twist can be calculated.

Now the torsional stiffness of the wing at any spanwise station can be represented either by the quantity $GJ$ or by the quantity $m_\theta$, where

$$\left.\begin{aligned} GJ &\equiv \frac{T}{d\theta/dy} \\ m_\theta &\equiv \frac{T}{\theta} \end{aligned}\right\} \tag{7}$$

If the expression for GJ is integrated, then

$$\frac{\theta}{T} = \int_0^y \frac{dy}{GJ}$$

or

$$\frac{1}{m_\theta} = \int_0^y \frac{dy}{GJ} \tag{8}$$

so that if, for example,

$$\left.\begin{aligned} \frac{1}{GJ} &= k \\ \frac{1}{m_\theta} &= ky \end{aligned}\right\} \tag{9}$$

then

and if

$$\left.\begin{aligned} \frac{1}{GJ} &= ky^2 \\ \frac{1}{m_\theta} &= \frac{k}{3} y^3 \end{aligned}\right\} \tag{10}$$

then

These results are of use in the subsequent analysis.

Consider the parameter GJ. From equation (7)

$$\frac{d\theta}{dy} = \frac{T}{GJ} \tag{11}$$

Substitution of this expression in equation (6) makes possible the calculation of $\theta$ at any point along the span.

The twist was calculated for two assumed spanwise variations of torsional stiffness. The first $\frac{1}{GJ} = k$ $\left(\text{or } \frac{1}{m_\theta} \propto y\right)$ is known to be representative of many small-scale models used in free-flight supersonic research. The second $\frac{1}{GJ} = ky^2$ $\left(\text{or } \frac{1}{m_\theta} \propto y^3\right)$ is typical of many subsonic fighter aircraft. (The degree of applicability to future supersonic aircraft can only be conjectured.) The procedure outlined can be used to obtain equations for other stiffness distributions. The following equations are the results of the twist calculations: For $\frac{1}{GJ} = k$,

$$\frac{\theta}{kC_{p_\infty} qbc^3} = \frac{B}{2\beta} \frac{y}{s} \tag{12a}$$

where $0 \leqq \frac{y}{s} \leqq 1 - \frac{b_a}{b}$ and

$$\frac{\theta}{kC_{p_\infty} qbc^3} = \frac{B}{4\beta \frac{b_a}{b}} \left[ 2\frac{y}{s} - \left(\frac{y}{s}\right)^2 - \left(1 - \frac{b_a}{b}\right)^2 \right] \tag{12b}$$

where $1 - \frac{b_a}{b} \leqq \frac{y}{s} \leqq 1$. For $\frac{1}{GJ} = ky^2$,

$$\frac{\theta}{kC_{p_\infty} qb^3c^3} = \frac{B}{24\beta} \left(\frac{y}{s}\right)^3 \tag{13a}$$

where $0 \leqq \frac{y}{s} \leqq 1 - \frac{b_a}{b}$ and

$$\frac{\theta}{kC_{p_\infty} q b^3 c^3} = \frac{B}{96\beta \frac{b_a}{b}} \left[ 4 \left(\frac{y}{s}\right)^3 - 3 \left(\frac{y}{s}\right)^4 - \left(1 - \frac{b_a}{b}\right)^4 \right] \tag{13b}$$

where $1 - \frac{b_a}{b} \leqq \frac{y}{s} \leqq 1$.

The twist may be expressed more conveniently as the ratio of the twist $\theta$ at any station to the twist $\theta_r$ at a reference station, taken at the midspan of the aileron $\left(\frac{y}{s} = 1 - \frac{1}{2}\frac{b_a}{b}\right)$. From equations (12) for $\frac{1}{GJ} = k$,

$$\frac{\theta}{\theta_r} = \frac{2b_a/b}{R_1} \frac{y}{s} \tag{14a}$$

where $0 \leqq \frac{y}{s} \leqq 1 - \frac{b_a}{b}$ and

$$\frac{\theta}{\theta_r} = \frac{1}{R_1} \left[ 2 \frac{y}{s} - \left(\frac{y}{s}\right)^2 - \left(1 - \frac{b_a}{b}\right)^2 \right] \tag{14b}$$

where $1 - \frac{b_a}{b} \leqq \frac{y}{s} \leqq 1$. From equations (13) for $\frac{1}{GJ} = ky^2$,

$$\frac{\theta}{\theta_r} = \frac{4b_a/b}{R_2} \left(\frac{y}{s}\right)^3 \tag{15a}$$

where $0 \leqq \frac{y}{s} \leqq 1 - \frac{b_a}{b}$ and

$$\frac{\theta}{\theta_r} = \frac{1}{R_2}\left[4\left(\frac{y}{s}\right)^3 - 3\left(\frac{y}{s}\right)^4 - \left(1 - \frac{b_a}{b}\right)^4\right] \tag{15b}$$

where $1 - \frac{b_a}{b} \leq \frac{y}{s} \leq 1$.

Although these expressions for the twist are not complicated, the use of a single twist equation which applies over the entire span results in a considerable saving of effort when evaluating the rolling-moment loss due to twist. For this reason, equations (14) and (15) were approximated by the following expressions: For $\frac{1}{GJ} = k$ $\left(\text{or } \frac{1}{m_\theta} \propto y\right)$,

$$\frac{\theta}{\theta_r} = \frac{12 - 4\frac{b_a}{b}}{8 - 5\frac{b_a}{b}}\frac{y}{s} - \frac{4}{8 - 5\frac{b_a}{b}}\left(\frac{y}{s}\right)^2 \tag{16a}$$

where $0 \leq \frac{y}{s} \leq 1$ and for $\frac{1}{GJ} = ky^2$ $\left(\text{or } \frac{1}{m_\theta} \propto y^3\right)$,

$$\frac{\theta}{\theta_r} = \frac{1}{\left(1 - \frac{1}{2}\frac{b_a}{b}\right)^2}\left(\frac{y}{s}\right)^2 \tag{16b}$$

where $0 \leq \frac{y}{s} \leq 1$. These approximations are compared with equations (14) and (15) in figure 3 for two values of $b_a/b$.

Rolling-moment-loss coefficient $\beta C_{l_{\theta_r}}$.- With the twist evaluated, there remains the problem of determining the rolling moment resulting from the twist. Equations (16a) and (16b) can be rewritten, respectively, as

$$\theta = \left( \frac{2}{b} \frac{12 - 4\frac{b_a}{b}}{8 - 5\frac{b_a}{b}} \theta_r \right) y - \left( \frac{4}{b^2} \frac{4}{8 - 5\frac{b_a}{b}} \theta_r \right) y^2 \tag{17a}$$

$$\theta = \left[ \frac{4}{b^2} \frac{\theta_r}{\left( 1 - \frac{1}{2} \frac{b_a}{b} \right)^2} \right] y^2 \tag{17b}$$

from which the twist is seen to be represented by two components, one linear with respect to $y$ and the other parabolic with respect to $y$. The rolling-moment coefficient resulting from a linear twist has been evaluated in reference 4 and may be written as

$$\beta C_l = \frac{w_1}{V} \frac{b}{2} \frac{2}{3} \left[ 1 - \frac{3}{2} \frac{1}{\beta A} + \frac{1}{2} \frac{1}{(\beta A)^2} + \frac{1}{8} \frac{1}{(\beta A)^3} \right] \tag{18}$$

where $w_1/V$ is the coefficient of the y-term in the twist equation. The rolling-moment coefficient due to a parabolic twist is derived in the appendix and is

$$\beta C_l = \frac{w_2}{V} \frac{b^2}{4} \frac{1}{2} \left[ 1 - \frac{2}{\beta A} + \frac{5}{3} \frac{1}{(\beta A)^2} - \frac{1}{2} \frac{1}{(\beta A)^3} - \frac{1}{8} \frac{1}{(\beta A)^4} \right] \tag{19}$$

where $w_2/V$ is the coefficient of the $y^2$-term in the twist equation. If the expressions for $w_1/V$ and $w_2/V$ from equations (17a) and (17b) are substituted in equations (18) and (19) and if the derivative is taken with respect to $\theta_r$, then after some simplification the following equations result for $\frac{1}{GJ} = k \left( \text{or } \frac{1}{m_\theta} \propto y \right)$,

$$\beta C_{l_{\theta_r}} = \frac{4}{8 - 5\frac{b_a}{b}}\left[\frac{3}{2} - \frac{2}{\beta A} + \frac{1}{6}\frac{1}{(\beta A)^2} + \frac{1}{2}\frac{1}{(\beta A)^3} + \frac{1}{16}\frac{1}{(\beta A)^4}\right]$$

$$- \frac{4\frac{b_a}{b}}{8 - 5\frac{b_a}{b}}\left[\frac{2}{3} - \frac{1}{\beta A} + \frac{1}{3}\frac{1}{(\beta A)^2} + \frac{1}{12}\frac{1}{(\beta A)^3}\right] \tag{20}$$

and for $\frac{1}{GJ} = ky^2$ $\left(\text{or } \frac{1}{m_\theta} \propto y^3\right)$,

$$\beta C_{l_{\theta_r}} = \frac{1}{2\left(1 - \frac{1}{2}\frac{b_a}{b}\right)^2}\left[1 - \frac{2}{\beta A} + \frac{5}{3}\frac{1}{(\beta A)^2} - \frac{1}{2}\frac{1}{(\beta A)^3} - \frac{1}{8}\frac{1}{(\beta A)^4}\right] \tag{21}$$

Twist parameter $\theta_r/\delta$.— The twist parameter may be evaluated directly in terms of $m_{\theta_r}$, the torsional stiffness at the reference station (aileron midspan), from equations (12) and (13). The value of $k$ is found from equations (9) and (10), and if the value of $C_p$ is taken conservatively as $4\delta/\beta$ (the linearized-theory result), then the following expressions are obtained: For $\frac{1}{m_\theta} \propto y$ $\left(\text{or } \frac{1}{GJ} = k\right)$,

$$\frac{\theta_r}{\delta} = \frac{b^3}{m_{\theta_r}}\frac{\beta q}{(\beta A)^3}\frac{2BR_1}{\frac{b_a}{b}\left(1 - \frac{1}{2}\frac{b_a}{b}\right)} \tag{22}$$

and for $\frac{1}{m_\theta} \propto y^3$ $\left(\text{or } \frac{1}{GJ} = ky^2\right)$,

$$\frac{\theta_r}{\delta} = \frac{b^3}{m_{\theta_r}} \frac{\beta q}{(\beta A)^3} \frac{BR_2}{\frac{b_a}{b}\left(1 - \frac{1}{2}\frac{b_a}{b}\right)^3} \tag{23}$$

## COMPUTATION PROCEDURE AND DISCUSSION

The solution of equations (2) and (3) is most easily carried out with the aid of a computation form such as that shown in table I, which is largely self-explanatory. The various quantities to be entered in the computation form are read from figures 4 to 11; in figures 6 to 11 is noted the source of the data presented. The quantity $\beta A$, which is the abscissa for most of the figures, is found from figure 5 for any value of Mach number and aspect ratio. The quantity $\beta q$ can be found either directly from table II for certain selected altitudes or from table II and figure 4 for intermediate altitudes.

The determination of the rolling-moment-effectiveness coefficient $\beta C_{l_\delta}$ requires some discussion. When $F = 1$ the values of $\beta C_{l_\delta}/F$ given in figure 6 represent linearized-theory values. The quantity $F$ (see fig. 7) is a reduction factor which takes into account the finite trailing-edge angle of the aileron. The value of $F$ was obtained by taking the value for the first two terms of the thickness reduction factor given in figure 4 of reference 3. Some recent experimental evidence indicates that, presumably because of boundary-layer effects, the use of the first two terms gives results which are in closer agreement with experimental data than are results obtained by using the complete three terms. Although the factor $F$ is strictly applicable only to flat-sided ailerons, it can be applied to other ailerons with little loss in over-all accuracy by estimating an effective trailing-edge angle.

An explicit solution for the reversal speed is difficult because of the manner in which $\beta A$ enters the quantities involved. The reversal speed may be found by a method similar to the one used in reference 5 to indicate divergence speed. Often, however, the variation of the rate of roll through the speed range is of more interest than the reversal speed alone; if this variation is calculated by use of table I, the reversal speed is automatically given, if reversal occurs. Because of the linear dependence of $\theta_r/\delta$ on $1/m_{\theta_r}$ and $q$, the values of $\frac{pb/2V}{(pb/2V)_R}$ found

from table I for specified values of stiffness and altitude can be converted easily to give results for other values of stiffness and altitude.

Often a solution is desired for the torsional stiffness required to maintain a certain percentage of the rate of roll that would be obtained with a rigid wing. This solution is easily effected by a slight rearrangement of the last several columns of table I, as shown in the table.

As an example of the type of data obtained from the use of the figures and the computation form, figure 12 shows the results of some computations for a typical free-flight research model.

## CONCLUDING REMARKS

An analysis has been presented of the problem of the loss in rolling effectiveness at supersonic flight speeds for the case of the rectangular wing. The effects of the loss in lift in the various Mach cones were considered in the analysis, and equations were obtained for two assumed variations of the spanwise distribution of torsional stiffness.

A computation form and figures were prepared; with the aid of these, calculations can be made without the necessity of referring to the details of the analysis.

Langley Aeronautical Laboratory
National Advisory Committee for Aeronautics
Langley Field, Va., September 21, 1948

## APPENDIX

## ROLLING MOMENT RESULTING FROM PARABOLIC TWIST

If the pressure distribution over the twisted wing can be found, this pressure distribution may be integrated to give the rolling moment. Perhaps the most direct way to find the pressure distribution for the particular case in the present paper is to consider the twisted wing to be represented by a distribution of sources and sinks, so that the pressure distribution can be found by use of the methods of references 6 and 7.

In general, only one wing panel need be considered (see fig. 13). The distribution of vertical velocity along the span of this panel is just $w_2\eta^2$, where $w_2$ is a constant; on the other panel the distribution is $-w_2\eta^2$. At any point located between the Mach cones from the tip and center of the wing (see fig. 13(a)), the velocity potential on one surface is given by

$$\phi_1(x,y) = -\frac{w_2}{\pi}\int_{\eta_1}^{y}\int_{0}^{\xi_1} \eta^2 f(\xi,\eta)\, d\xi\, d\eta - \frac{w_2}{\pi}\int_{y}^{\eta_3}\int_{0}^{\xi_3} \eta^2 f(\xi,\eta)\, d\xi\, d\eta \qquad (A1)$$

where

$$f(\xi,\eta) = \left[(x-\xi)^2 - \beta^2(y-\eta)^2\right]^{-1/2}$$

At any point located within the tip Mach cone, the velocity potential is given by

$$\phi_2(x,y) = \phi_1(x,y) + \frac{w_2}{\pi}\int_{\eta_2}^{s}\int_{0}^{\xi_2} \eta^2 f(\xi,\eta)\, d\xi\, d\eta$$

$$+ \frac{w_2}{\pi}\int_{s}^{\eta_3}\int_{0}^{\xi_3} \eta^2 f(\xi,\eta)\, d\xi\, d\eta \tag{A2}$$

where the last two terms represent the effect of the finite tip. At any point within the Mach cone from the center of the wing, the velocity potential is

$$\phi_3(x,y) = \phi_1(x,y) + \frac{2w_2}{\pi}\int_{\eta_1}^{0}\int_{0}^{\xi_1} \eta^2 f(\xi,\eta)\, d\xi\, d\eta \tag{A3}$$

where the last term represents the effect of the opposite wing panel.

If a pressure coefficient is defined as

$$C_p \equiv \frac{P}{q} \tag{A4}$$

where $P$ is the lifting pressure, then

$$C_p = -\frac{4}{V}\frac{\partial \phi}{\partial x} \tag{A5}$$

When equations (A1), (A2), and (A3) are substituted in equation (A5) and the indicated operations are performed, the pressure distribution over the region between the Mach cones from the tip and center of the wing becomes

$$C_{p_1} = \frac{w_2}{V} \frac{2x^2 + 4\beta^2 y^2}{\beta^3} \tag{A6}$$

the pressure distribution over the part of the wing within the tip Mach cone is given by

$$C_{p_2} = \frac{w_2}{\pi V} \left[ \frac{2x^2 + 4\beta^2 y^2}{\beta^3} \cos^{-1} \frac{2\beta y - 2\beta s + x}{x} \right.$$

$$\left. - \frac{4\beta y + 4\beta s - 2x}{\beta^3} \sqrt{x^2 - \beta^2 \left( 2y - 2s + \frac{x}{\beta} \right)^2} \right] \tag{A7}$$

and in the center Mach cone the pressure distribution is

$$C_{p_3} = \frac{w_2}{\pi V} \left[ \frac{12y}{\beta^2} \sqrt{x^2 - \beta^2 y^2} + \frac{8\beta^2 y^2 + x^2}{\beta^3} \sin^{-1} \frac{\beta y}{x} \right] \tag{A8}$$

Now the rolling moment of one wing panel is simply

$$\frac{l_1}{q} = \int\int C_p y \, dy \, dx \tag{A9}$$

where the integration is taken over the area of the panel. The limits of integration are shown in figure 13(b). Equation (A9) becomes

$$\frac{l_1}{q} = \int_0^c \int_0^{x/\beta} C_{p_3} y \, dy \, dx + \int_0^c \int_{x/\beta}^{s-\frac{x}{\beta}} C_{p_1} y \, dy \, dx + \int_0^c \int_{s-\frac{x}{\beta}}^{s} C_{p_2} y \, dy \, dx \quad (A10)$$

These integrations, which, although tedious, can be carried out with the help of a table of integrals, give

$$\frac{l_1}{2q} \frac{\beta^3 V}{w_2} = \frac{1}{2}\beta^2 s^4 c - \frac{1}{2}\beta s^3 c^2 + \frac{5}{24} s^2 c^3 - \frac{1}{32} \frac{sc^4}{\beta} - \frac{21}{1280} \frac{c^5}{\beta^2}$$

The total rolling-moment coefficient is found by multiplying by 2 (for two panels) and dividing by $Sb = 4s^2c$. After a little simplification, the coefficient becomes

$$\beta C_l = \frac{w_2}{V} \frac{b^2}{4} \frac{1}{2} \left[ 1 - \frac{2}{\beta A} + \frac{5}{3} \frac{1}{(\beta A)^2} - \frac{1}{2} \frac{1}{(\beta A)^3} - \frac{1}{8} \frac{1}{(\beta A)^4} \right] \quad (A11)$$

which is equation (19).

## REFERENCES

1. Pearson, Henry A., and Aiken, William S., Jr.: Charts for the Determination of Wing Torsional Stiffness Required for Specified Rolling Characteristics or Aileron Reversal Speed. NACA Rep. No. 799, 1944.

2. Harmon, Sidney M.: Determination of the Effect of Wing Flexibility on Lateral Maneuverability and a Comparison of Calculated Rolling Effectiveness with Flight Results. NACA ARR No. 4A28, 1944.

3. Tucker, Warren A., and Nelson, Robert L.: Theoretical Characteristics in Supersonic Flow of Constant-Chord Partial-Span Control Surfaces on Rectangular Wings Having Finite Thickness. NACA TN No. 1708, 1948.

4. Harmon, Sidney M.: Stability Derivatives of Thin Rectangular Wings at Supersonic Speeds. Wing Diagonals Ahead of Tip Mach Lines. NACA TN No. 1706, 1948.

5. Diederich, Franklin W., and Budiansky, Bernard: Divergence of Swept Wings. NACA TN No. 1680, 1948.

6. Puckett, Allen E.: Supersonic Wave Drag of Thin Airfoils. Jour. Aero. Sci., vol. 13, no. 9, Sept. 1946, pp. 475-484.

7. Evvard, John C.: Distribution of Wave Drag and Lift in the Vicinity of Wing Tips at Supersonic Speeds. NACA TN No. 1382, 1947.

TABLE I

COMPUTATION FORM

$\left[\frac{b_a}{b} = \text{\_\_\_\_};\ \frac{c_m}{c} = \text{\_\_\_\_};\ A = \text{\_\_\_\_};\ \frac{l}{\rho g} = \text{\_\_\_\_};\ m_{\theta_r} = \text{\_\_\_\_}\ \text{ft-lb/radian};\ b = \text{\_\_\_\_}\ \text{ft};\ \text{and}\ \frac{\rho b^3}{m_{\theta_r}} = \text{\_\_\_\_}.\right]$

| ① | ② | ③ | ④ | ⑤ | ⑥ | ⑦ | ⑧ | ⑨ | ⑩ | ⑪ | ⑫ | ⑬ | ⑭ | ⑮ | ⑯ | ⑰ | ⑱ | ⑲ | ⑳ | ㉑ |
|---|---|---|---|---|---|---|---|---|---|---|---|---|---|---|---|---|---|---|---|---|
| M | Altitude (ft) | $\rho_q/(\rho_q)_0$ | $(\rho_q)_0$ | $\rho_q$ | $\Delta A$ | | | | $\beta C_{l_\delta}/F$ | F | $\beta C_{l_\delta}$ | $-\beta C_{l_p}$ | $\beta C_{l_{\theta_r}}$ | $\frac{e_r}{\delta}\frac{m_{\theta_r}(\Delta A)^2}{b^3\rho_q}$ | $\theta_r/\delta$ | $\beta C_{l_{\theta_r}}\frac{\theta_r}{\delta}$ | | | $\frac{pb/2V}{\delta}$ | $\frac{pb/2V}{(pb/2V)_R}$ |
| Assumed | | Fig. 4 | Table II | ③ × ④ | Fig. 5 | ⑥² | ⑤/⑦ | ⑧ × $\frac{b^3}{m_{\theta_r}}$ | Fig. 6 | Fig. 7 | ⑩ × ⑪ | Fig. 8 | Fig. 9 | Fig. 10 or 11 | ⑮ × ⑨ | ⑭ × ⑯ | ⑱ − ⑰ | ⑰/⑮ | ⑱/⑬ | 1.0 − ⑲ |
| | | | | | | | | | | | | | | | | | | | | |
| | | | | | | | | | | | | | | | | | | | | |
| | | | | | | | | | | | | | | | | | | | | |
| | | | | | | | | | | | | | | | | | | | | |
| | | | | | | | | | | | | | | | | | | | | |
| | | | | | | | | | | | | | | | | | | | | |

Alternative arrangement, used for finding required torsional stiffness

| ⑯ | ⑰ | ⑱ | ⑲ | ⑳ | ㉑ |
|---|---|---|---|---|---|
| $\frac{pb/2V}{(pb/2V)_R}$ | | | $\theta_r/\delta$ | | $m_{\theta_r}$ |
| Assumed | 1.0 − ⑯ | ⑱/⑰ | ⑰ × ⑱ | $\frac{⑧ \times ⑲}{⑲}$ | ⑳ × $b^3$ |
| | | | | | |

TABLE II

$\beta$ AND $\beta q$ AS FUNCTIONS OF M

| M | $\beta$ | $\beta q$ for various altitudes | | | | | | |
|---|---|---|---|---|---|---|---|---|
| | | 0 | 10,000 ft | 20,000 ft | 30,000 ft | 40,000 ft | 50,000 ft | 60,000 ft |
| 1.1 | 0.458 | 821 | 564 | 377 | 244 | 152 | 94 | 59 |
| 1.2 | .663 | 1,414 | 973 | 650 | 420 | 262 | 162 | 101 |
| 1.3 | .831 | 2,080 | 1,430 | 956 | 617 | 386 | 239 | 148 |
| 1.4 | .980 | 2,845 | 1,956 | 1,307 | 845 | 527 | 327 | 203 |
| 1.5 | 1.118 | 3,726 | 2,562 | 1,712 | 1,106 | 690 | 428 | 266 |
| 1.6 | 1.249 | 4,736 | 3,256 | 2,176 | 1,405 | 877 | 545 | 337 |
| 1.7 | 1.375 | 5,886 | 4,047 | 2,705 | 1,746 | 1,090 | 677 | 419 |
| 1.8 | 1.497 | 7,184 | 4,940 | 3,301 | 2,132 | 1,331 | 825 | 512 |
| 1.9 | 1.616 | 8,641 | 5,942 | 3,971 | 2,565 | 1,600 | 992 | 616 |
| 2.0 | 1.732 | 10,262 | 7,056 | 4,715 | 3,045 | 1,900 | 1179 | 731 |
| 2.5 | 2.290 | 21,201 | 14,578 | 9,739 | 6,293 | 3,925 | 2437 | 1511 |
| 3.0 | 2.828 | 37,700 | 25,924 | 17,322 | 11,188 | 6,982 | 4332 | 2687 |
| 3.5 | 3.355 | 60,876 | 41,860 | 27,967 | 18,067 | 11,273 | 6995 | 4341 |

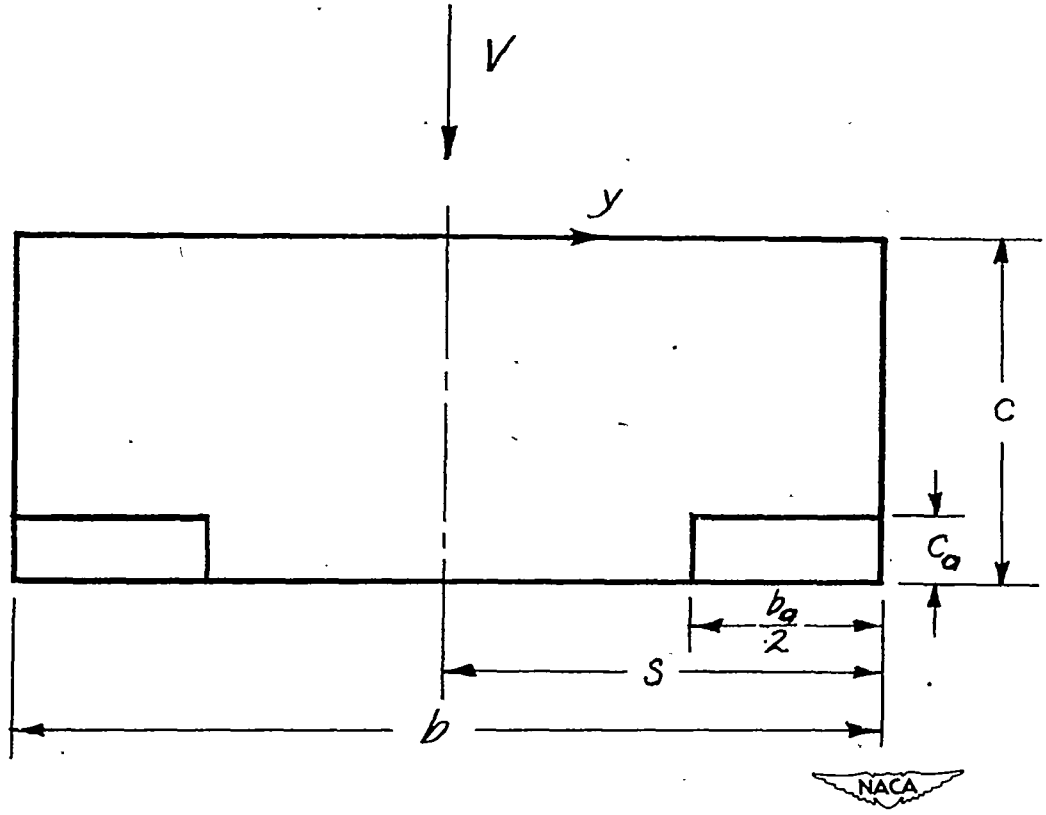


Figure 1.- The configuration investigated.

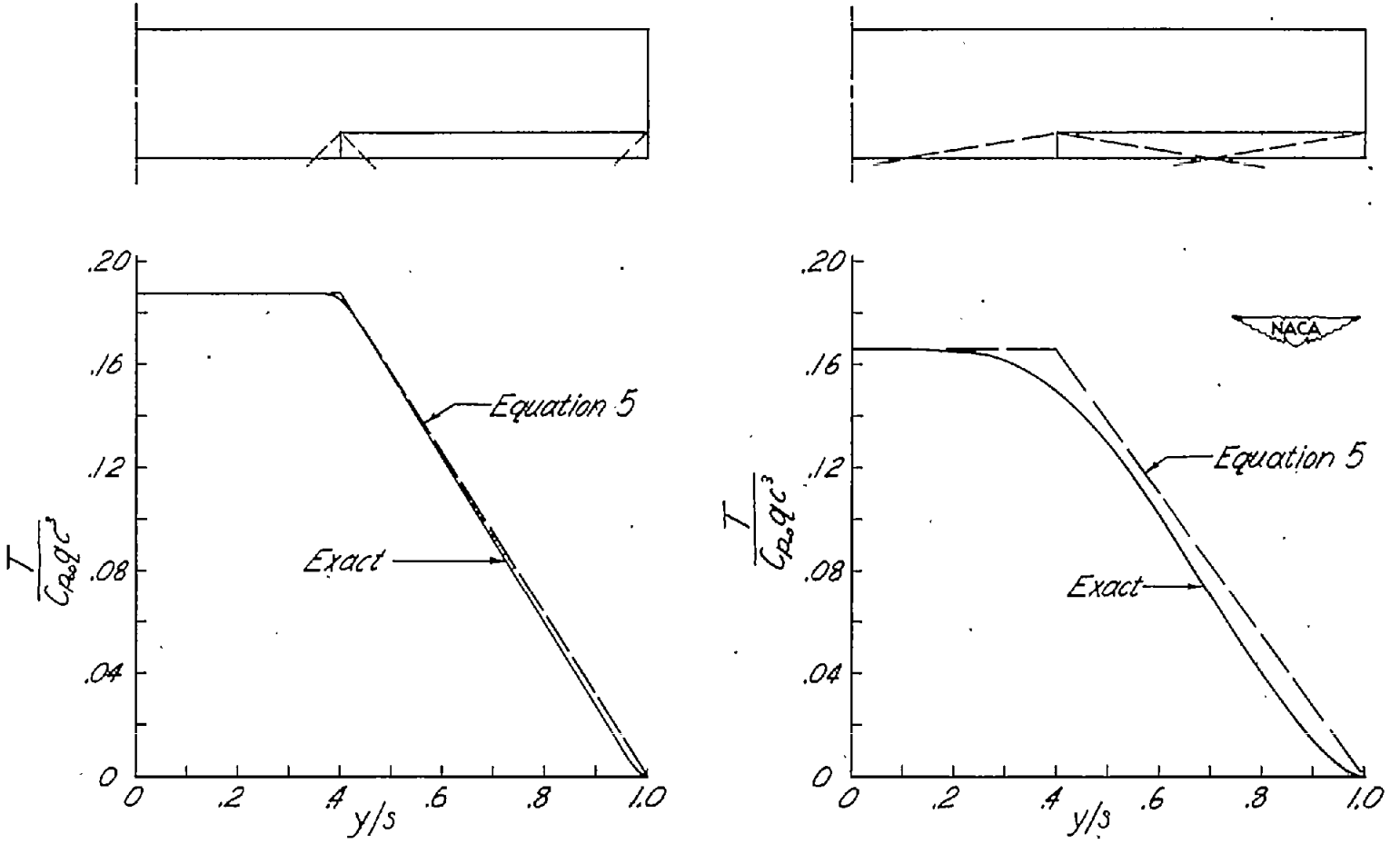


(a) $\beta = 1$.

(b) $\beta = \frac{1}{6}$.

Figure 2.- Comparison of exact and approximate torque distribution for a particular configuration. $A = 8$; $\frac{b_a}{b} = 0.6$; and $\frac{c_a}{c} = 0.2$.

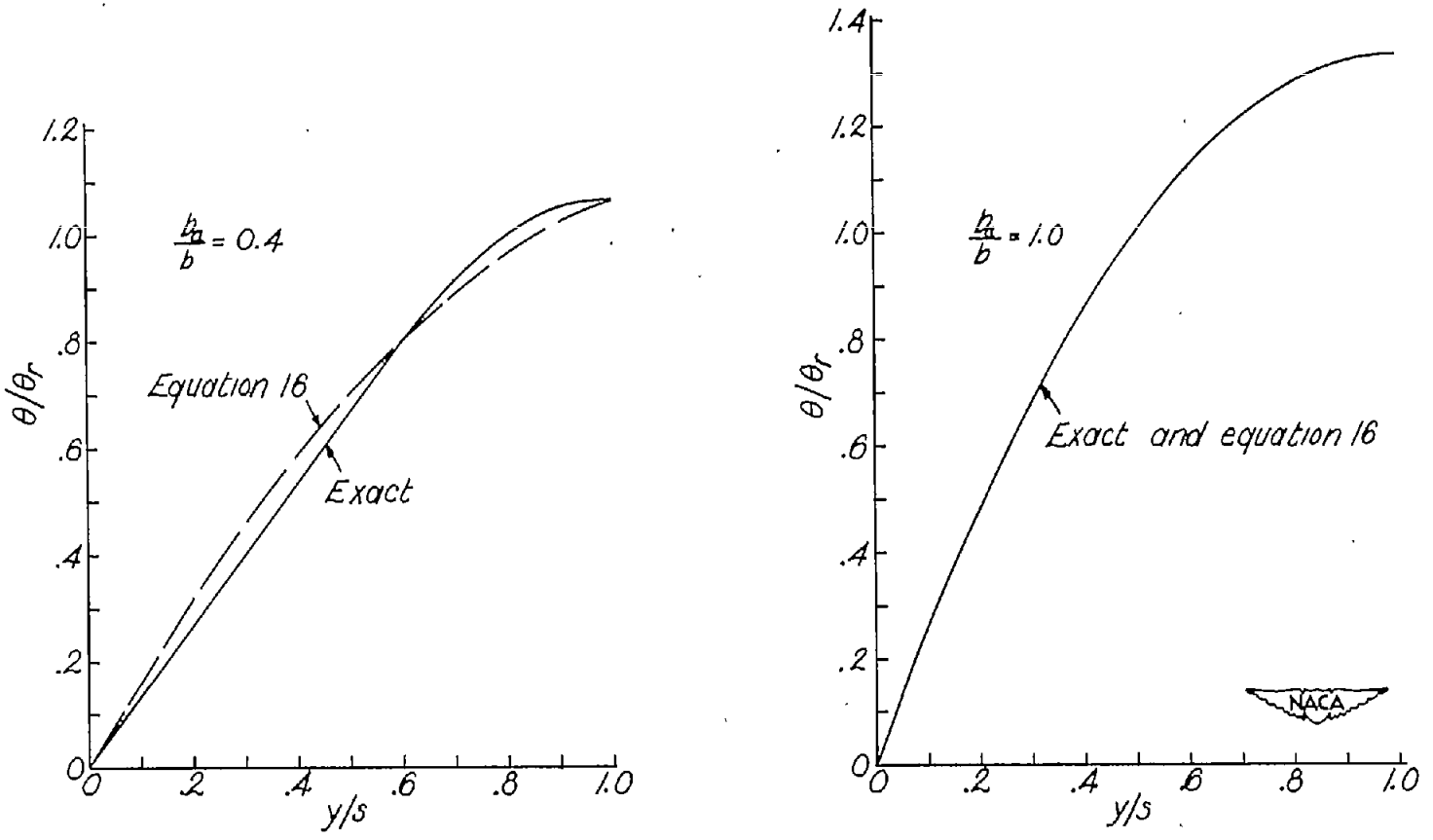


(a) $\frac{1}{m_\theta} \propto y$.

Figure 3.- Comparison of "exact" and approximate twist distribution. The "exact" results are based upon the approximate torque distribution shown in figure 2.

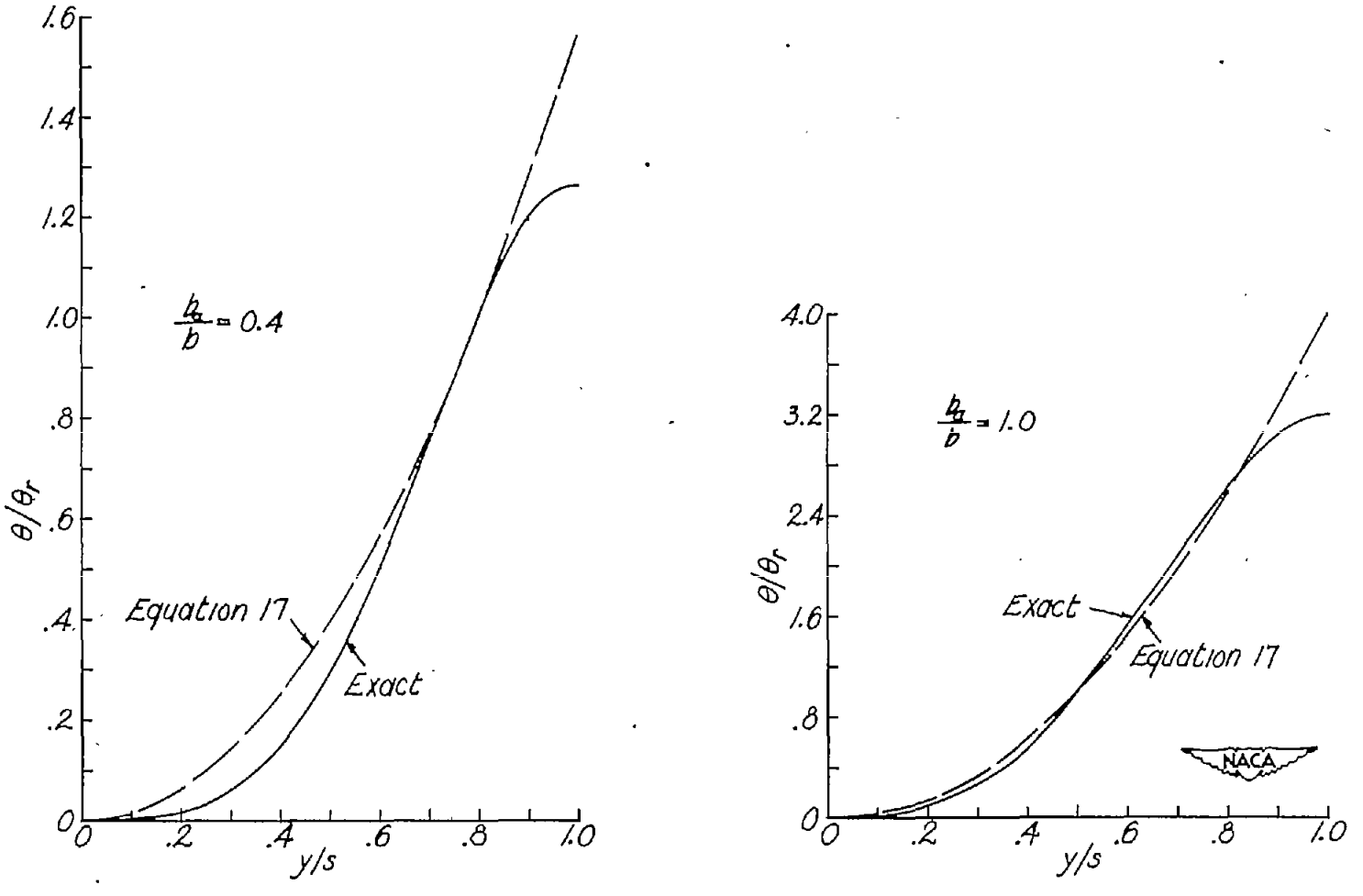


(b) $\frac{1}{m_\theta} \propto y^3$.

Figure 3.- Concluded.

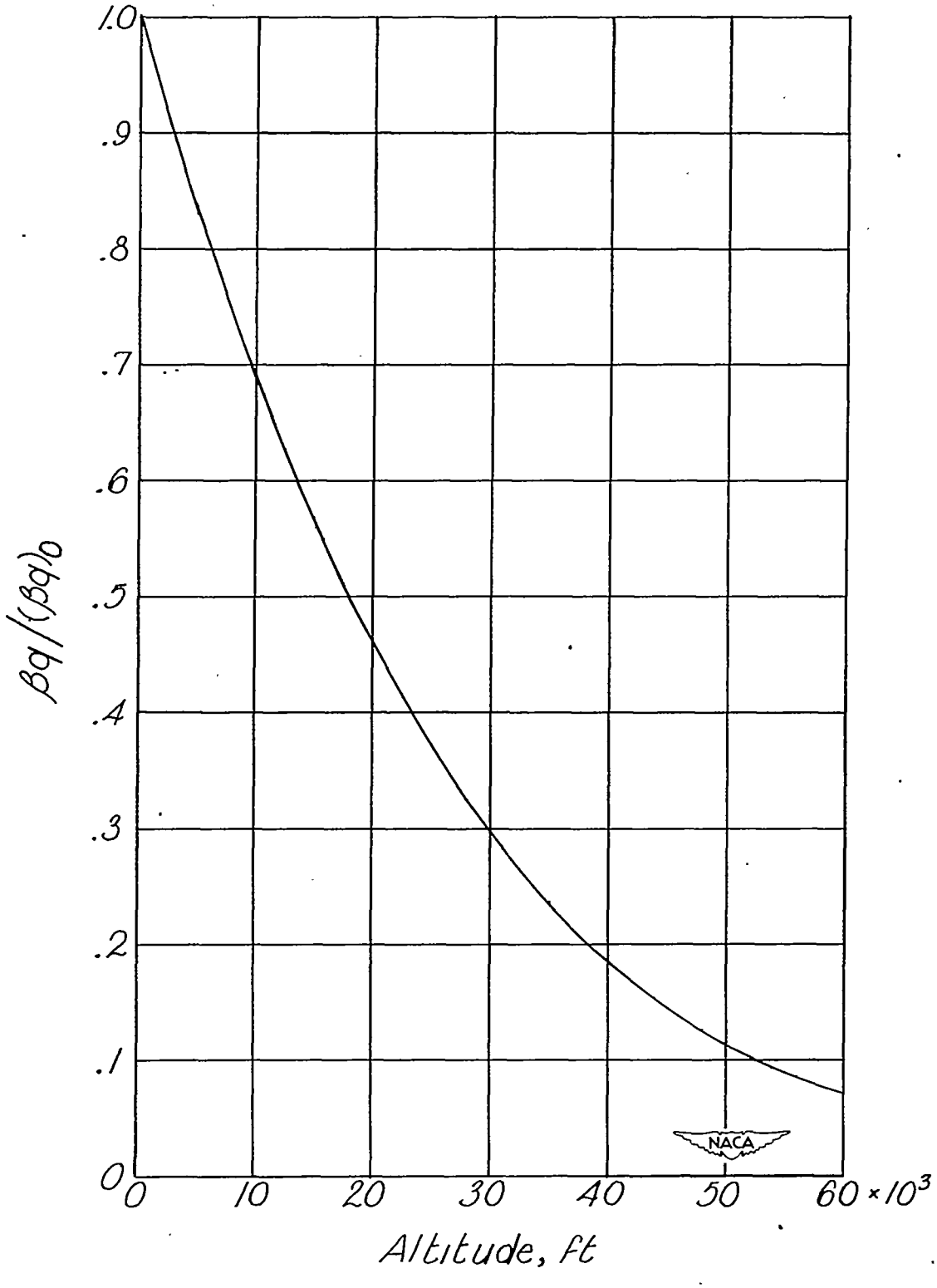


Figure 4.- Variation of dynamic-pressure ratio with altitude at constant Mach number.

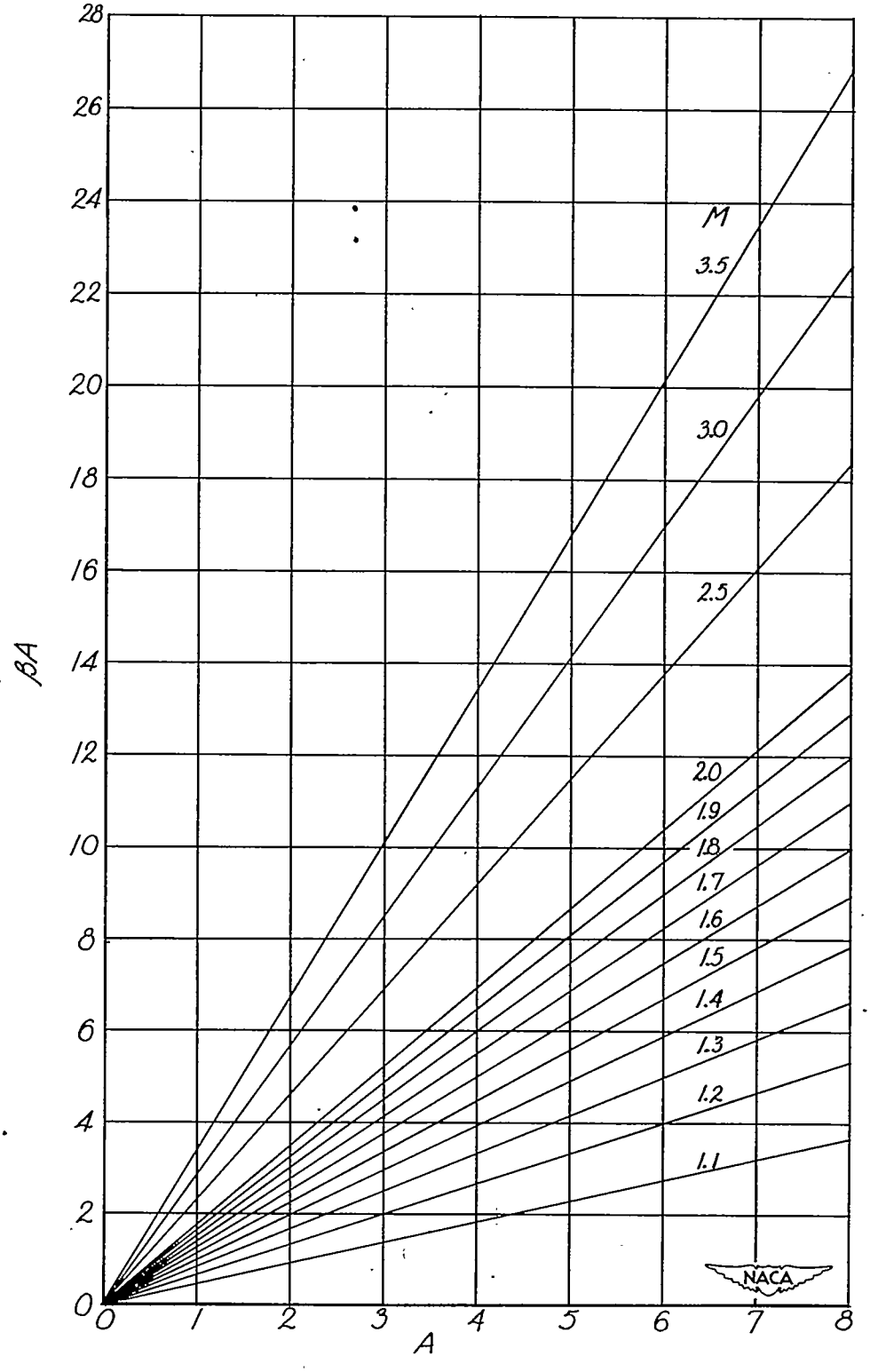


Figure 5.- Variation of βA with aspect ratio.

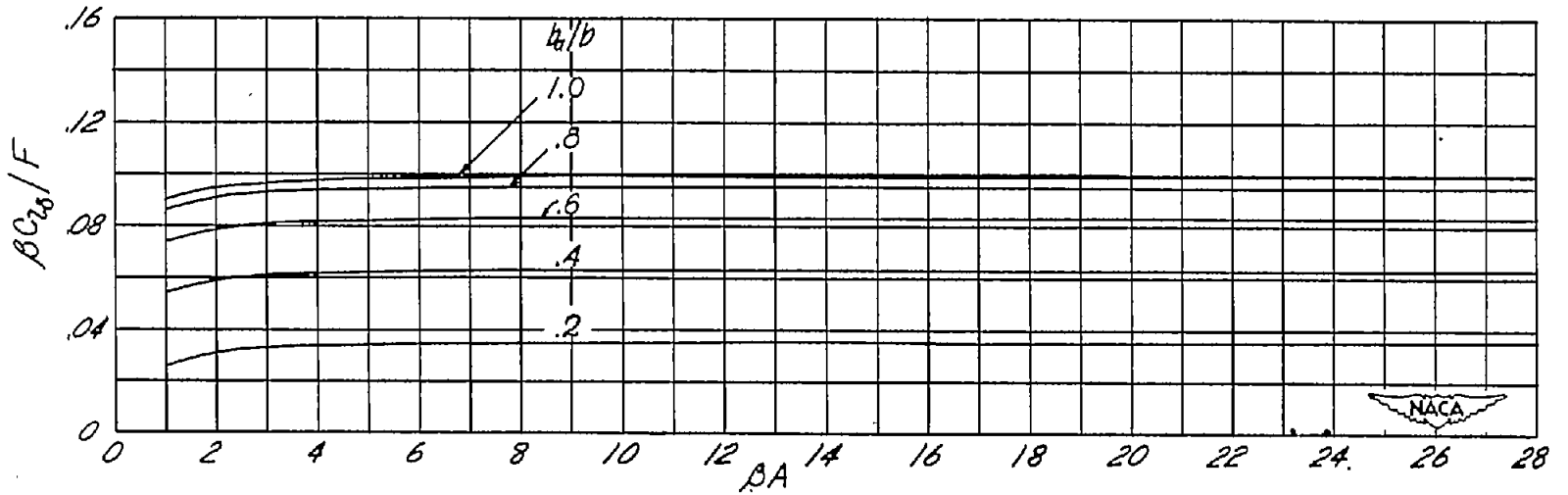


(a) $\frac{c_a}{c} = 0.1$.

Figure 6.- Variation of rolling-moment-effectiveness coefficient with βA. (From reference 3. See section entitled "Computation Procedure and Discussion" of present paper.)

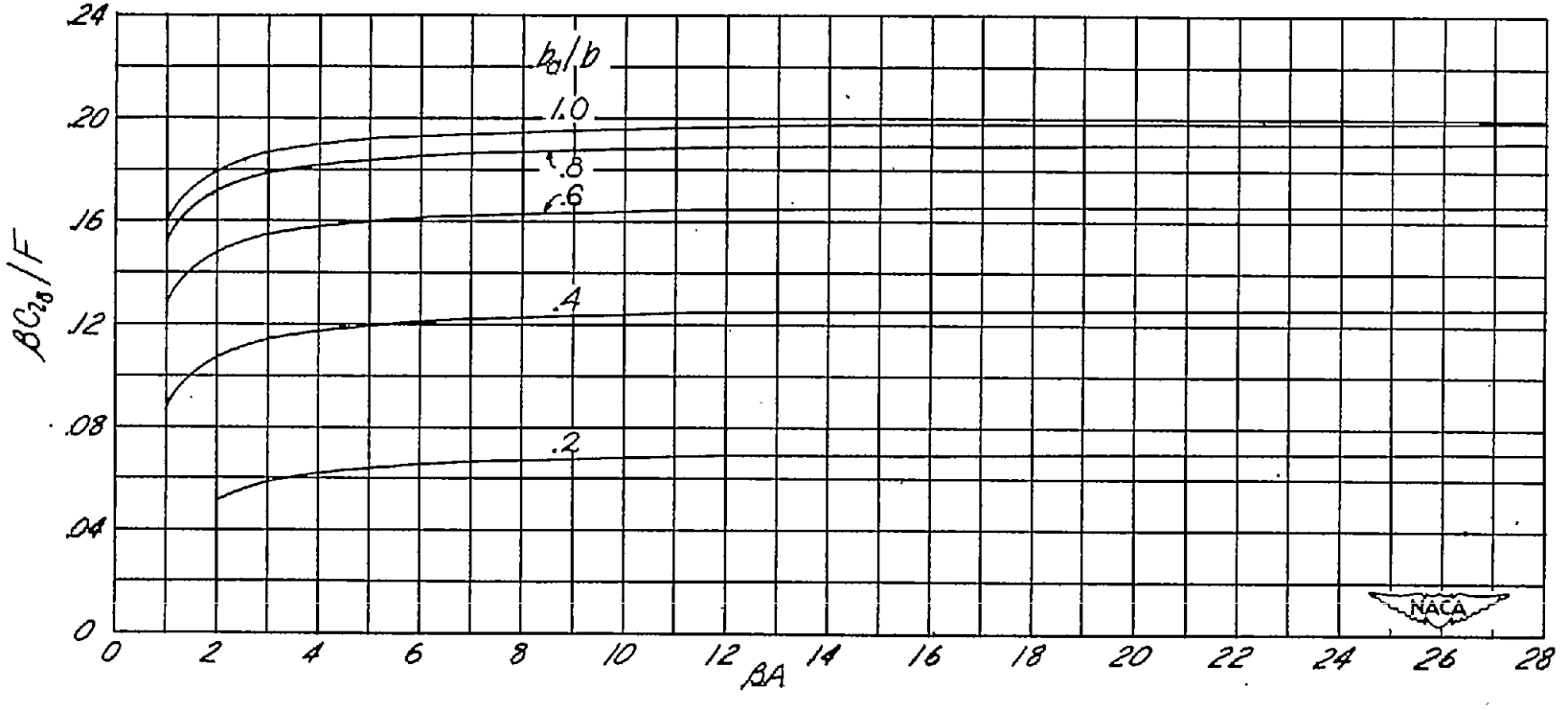


(b) $\frac{c_a}{c} = 0.2$.

Figure 6.- Continued.

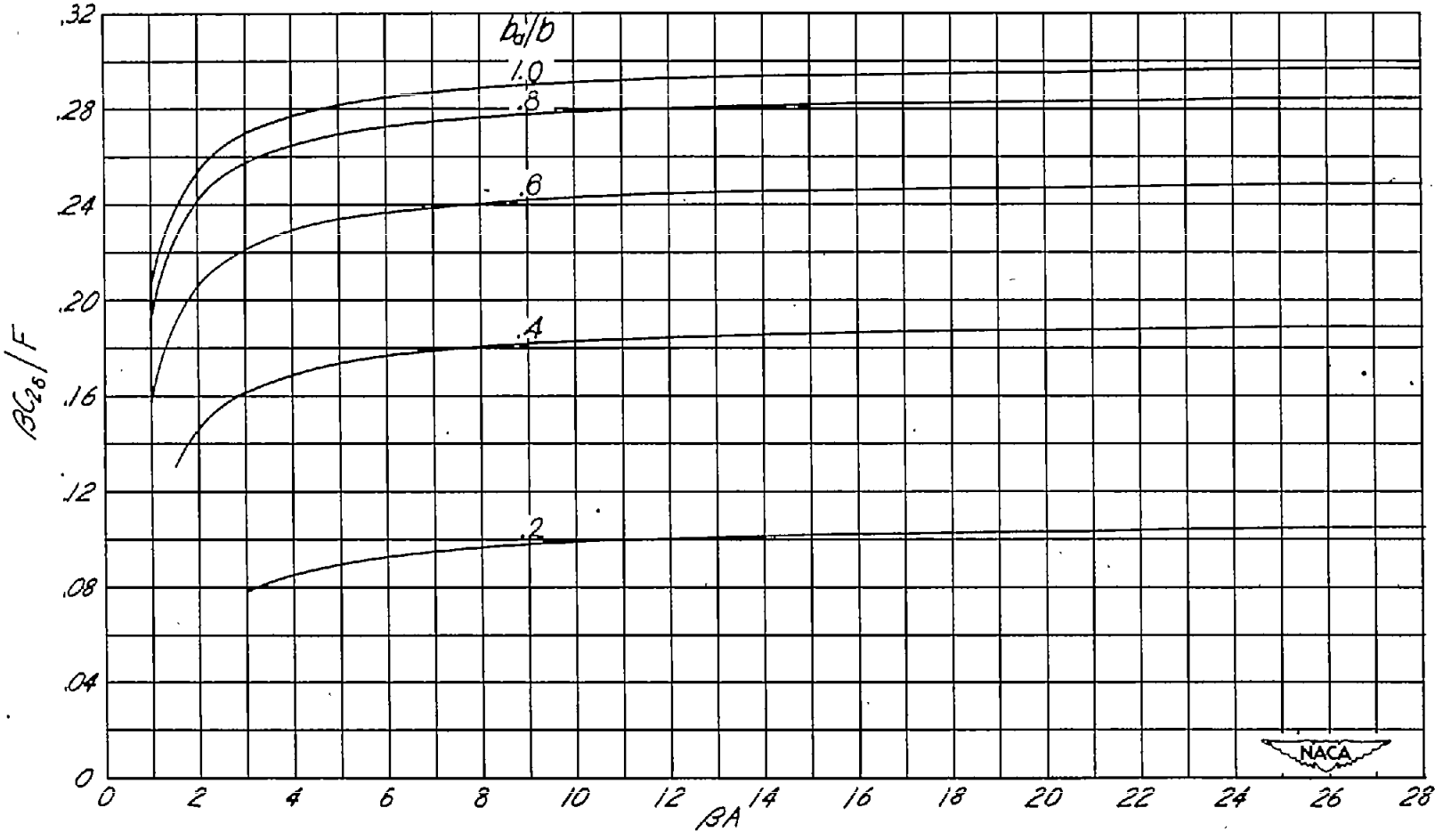


(c) $\frac{c_a}{c} = 0.3$.

Figure 6.- Concluded.

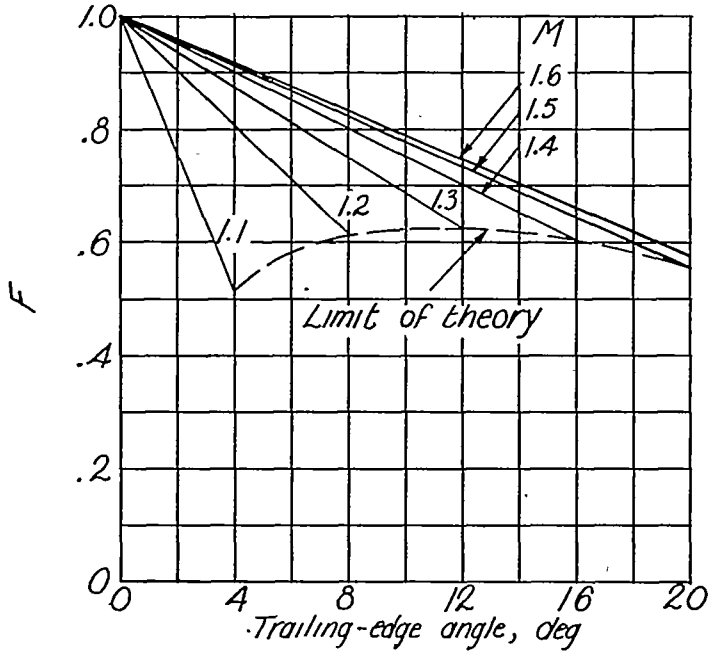


(a) $1.1 \leq M \leq 1.6$.

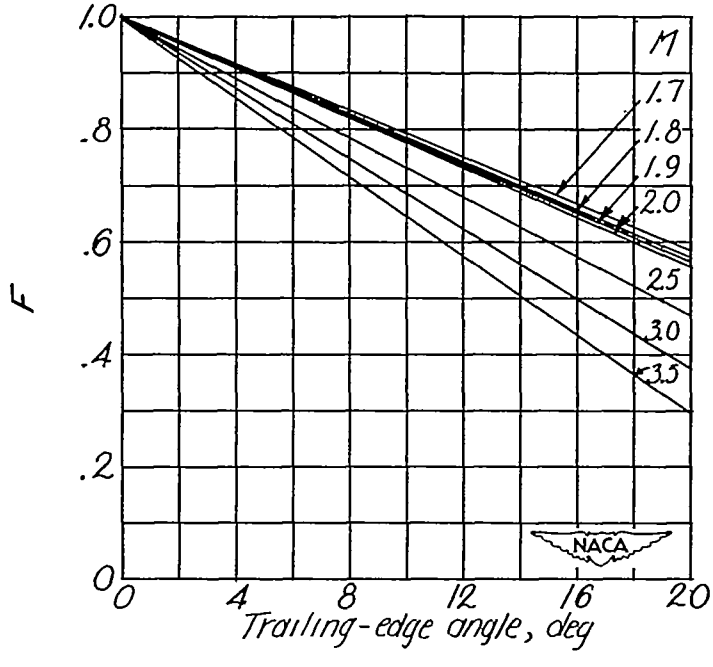


(b) $1.7 \leq M \leq 3.5$.

Figure 7.- Trailing-edge-angle reduction factor. (From reference 3. See section entitled "Computation Procedure and Discussion" of present paper.)

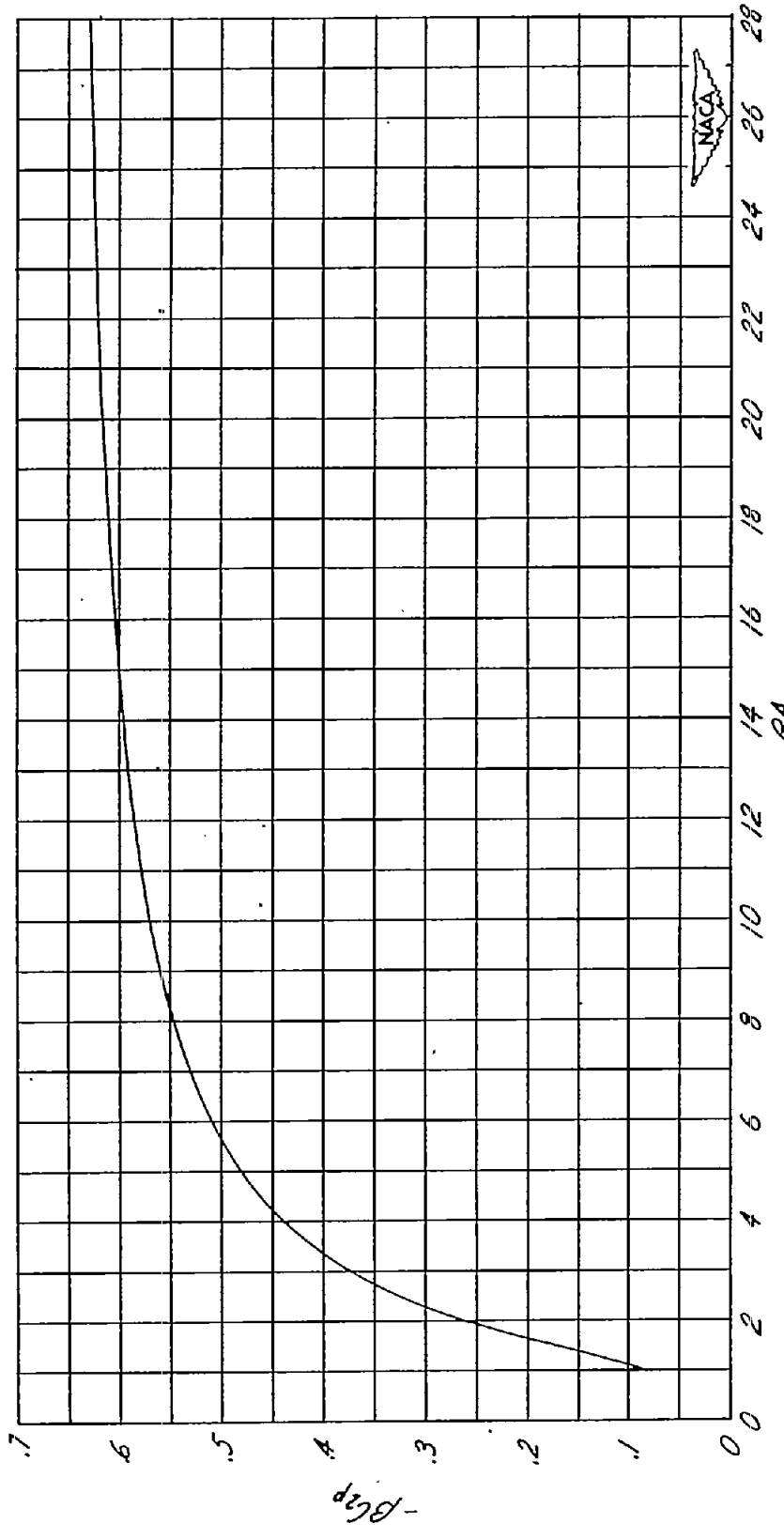


Figure 8.- Variation of damping-in-roll coefficient with βA. (From reference 4.)

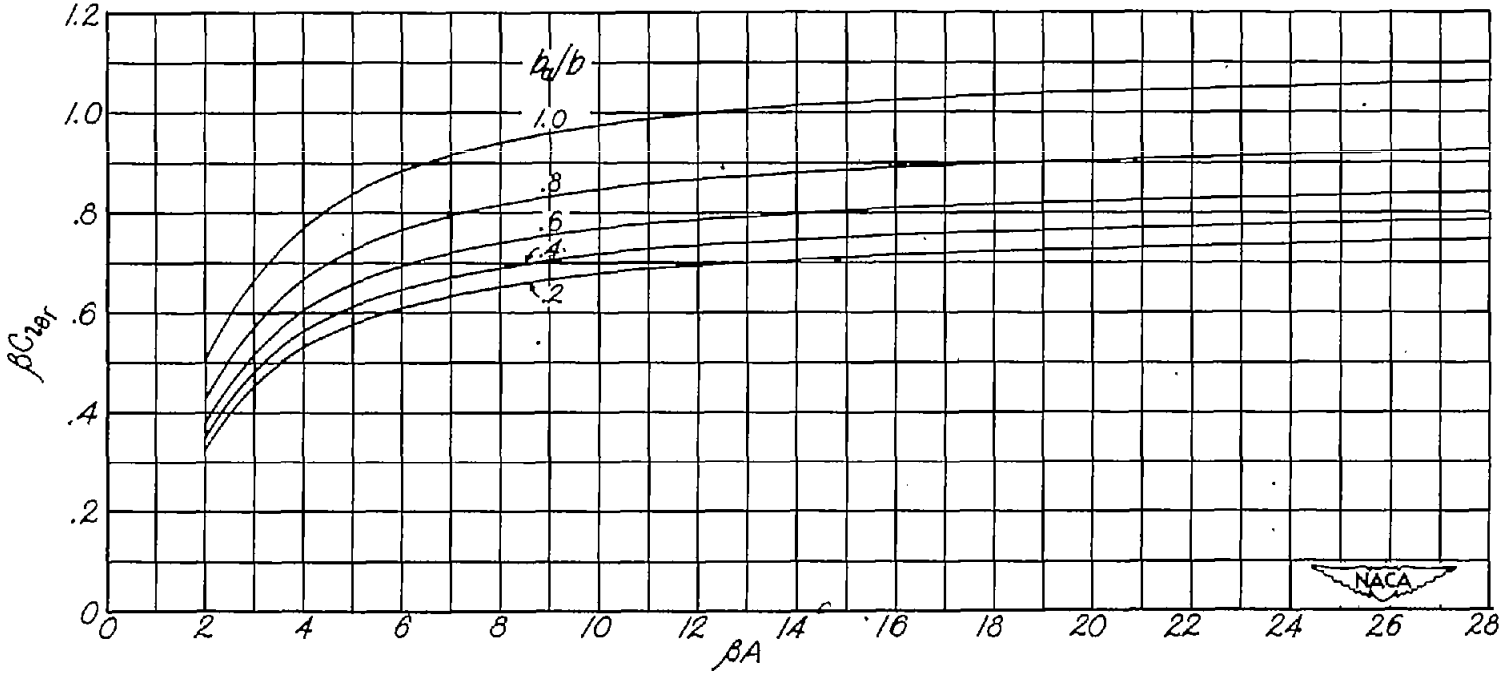


(a) $\frac{1}{m_\theta} \propto y$.

Figure 9.- Variation of rolling-moment-loss coefficient with $\beta A$. (From equations (20) and (21).)

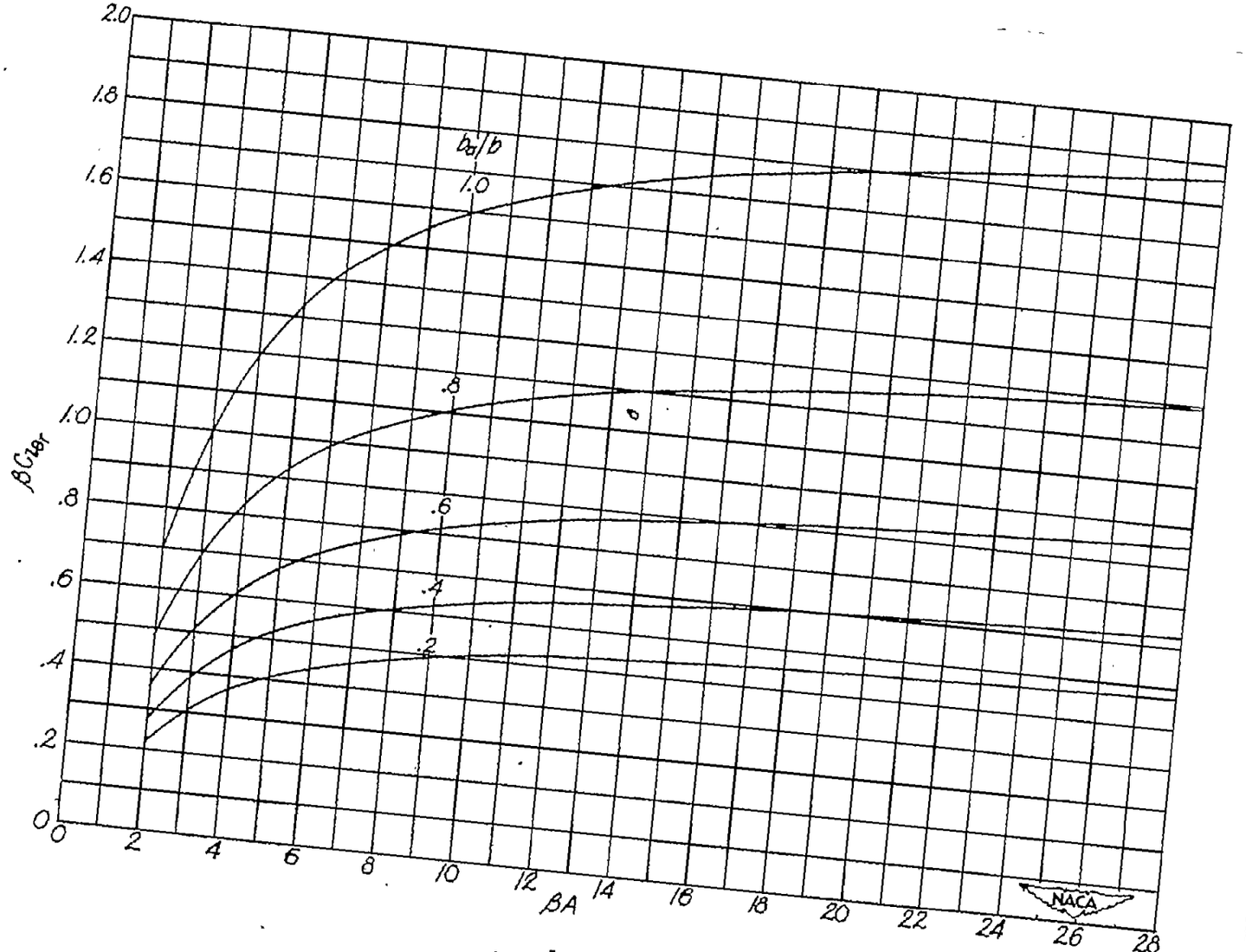


(b) $\frac{1}{m_\theta} \propto y^3$.

Figure 9.- Concluded.

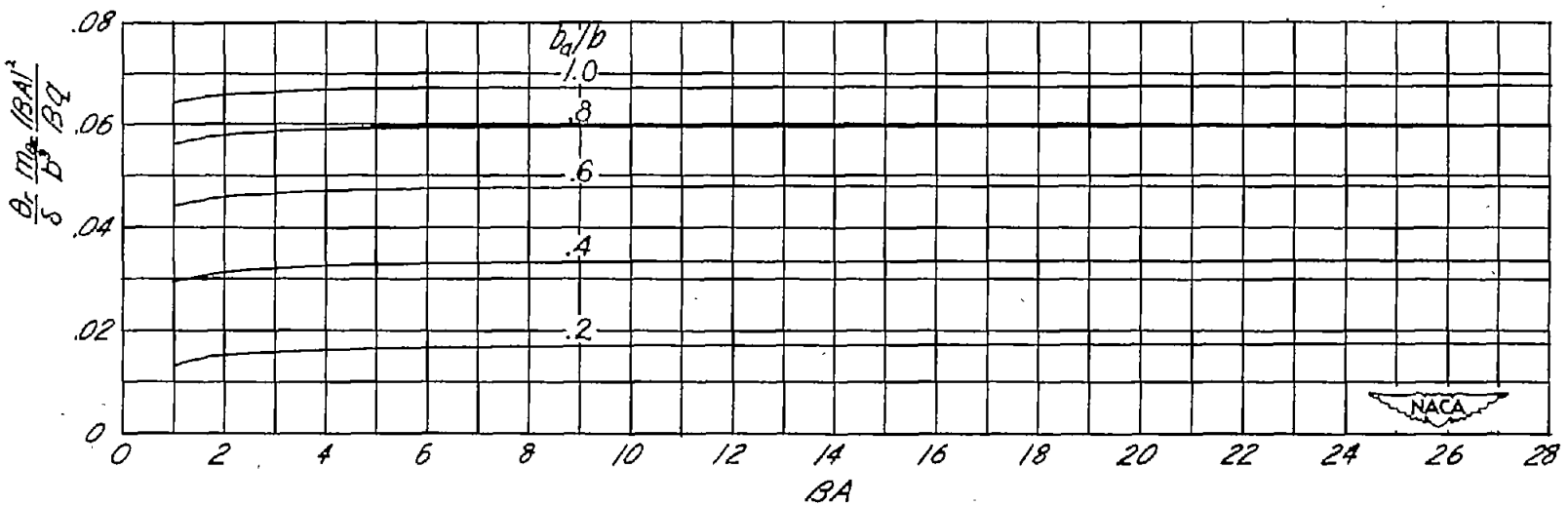


(a) $\frac{c_a}{c} = 0.1$.

Figure 10.- Variation of twist parameter with βA. $\frac{1}{m_\theta} \propto y$. (From equation (22).)

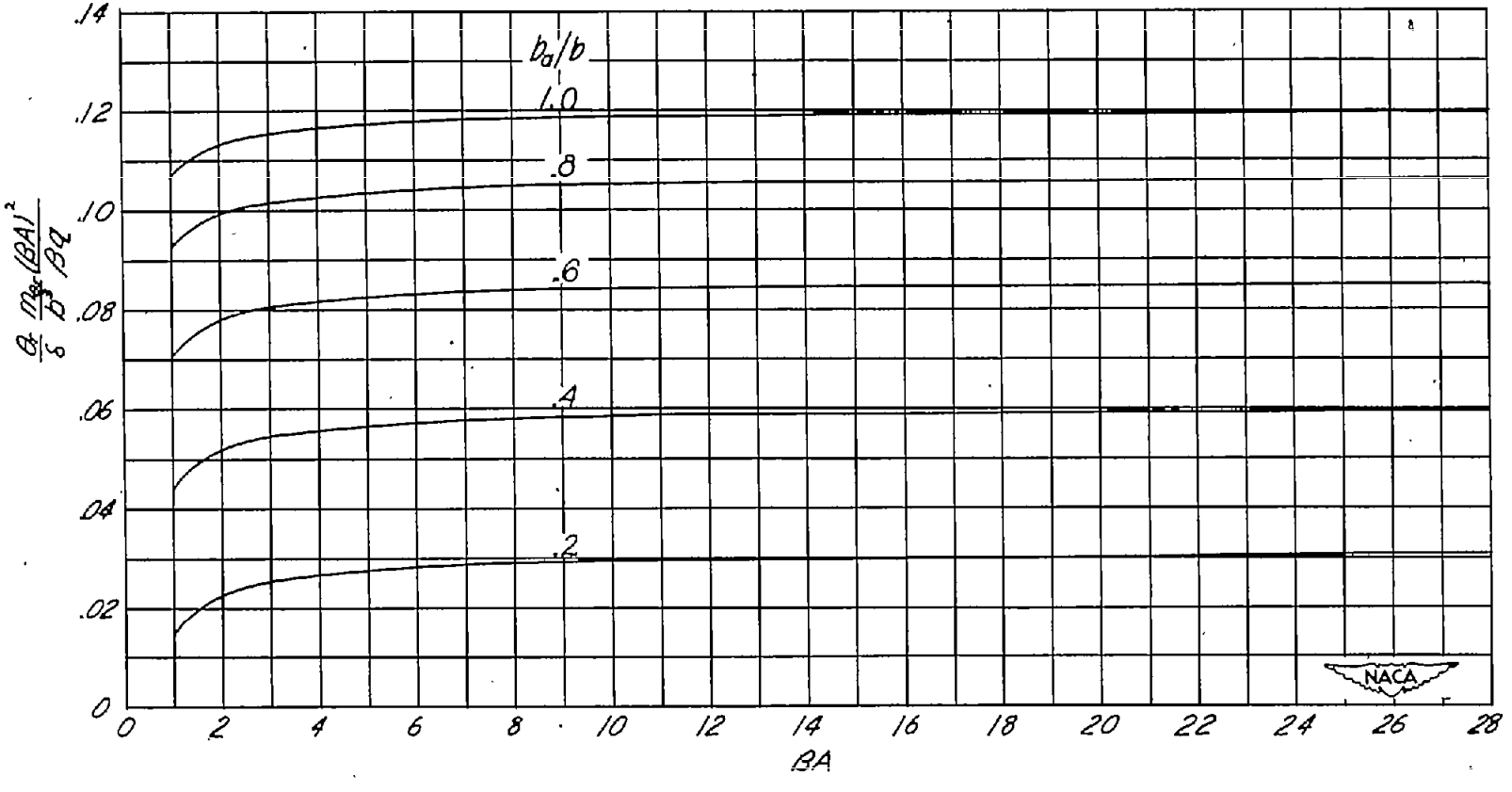


(b) $\frac{c_a}{c} = 0.2$.

Figure 10.- Continued.

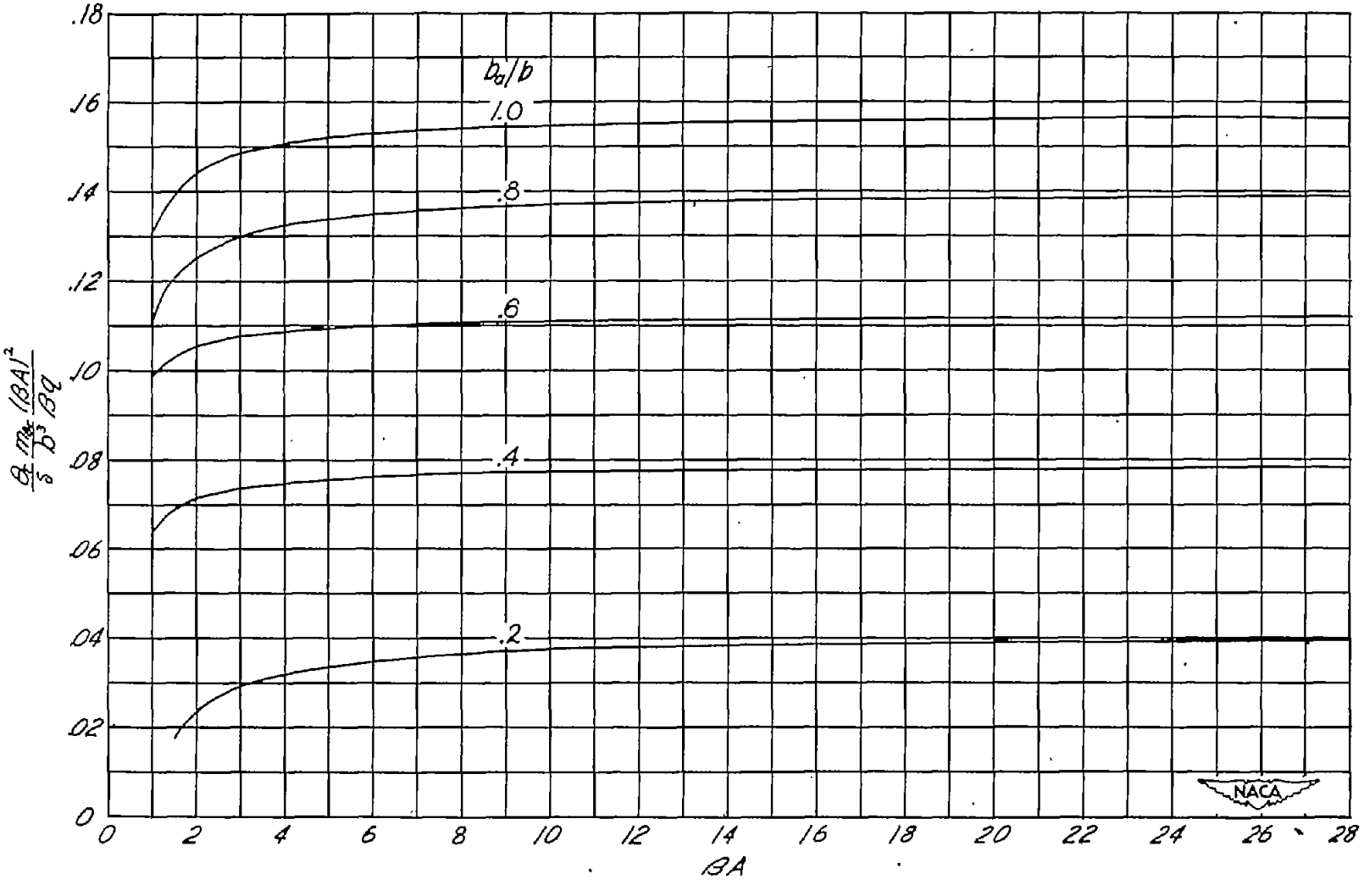


(c) $\frac{c_a}{c} = 0.3$.

Figure 10.- Concluded.

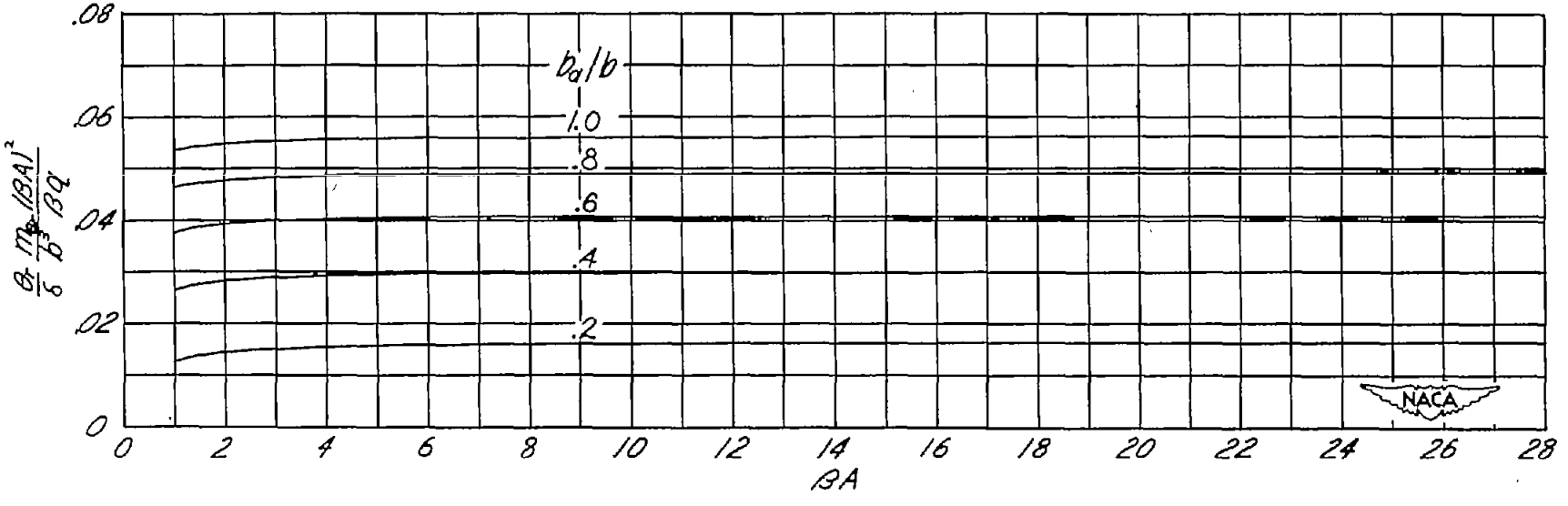


(a) $\frac{c_a}{c} = 0.1$.

Figure 11.- Variation of twist parameter with βA. $\frac{1}{m_\theta} \propto y^3$. (From equation (23).)

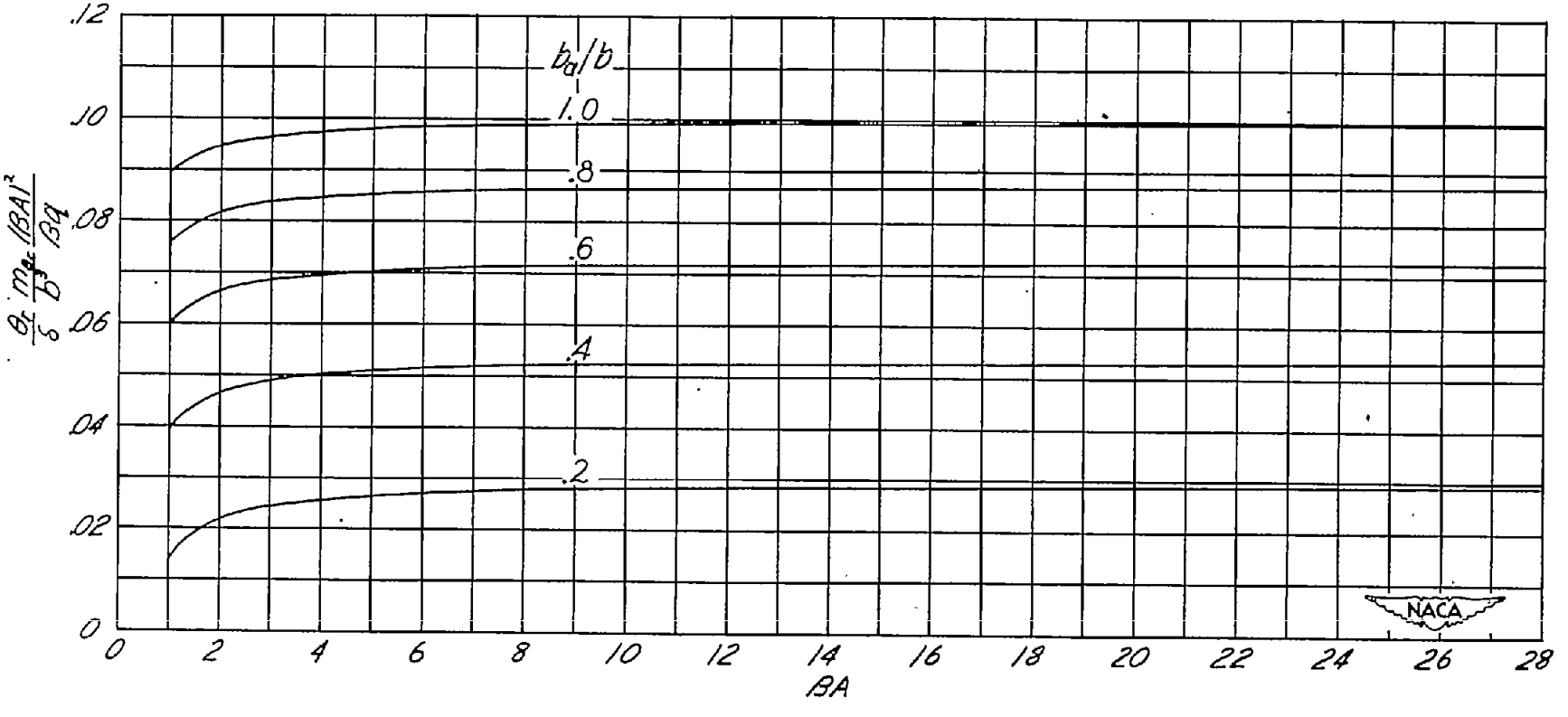


(b) $\frac{c_a}{c} = 0.2$.

Figure 11.- Continued.

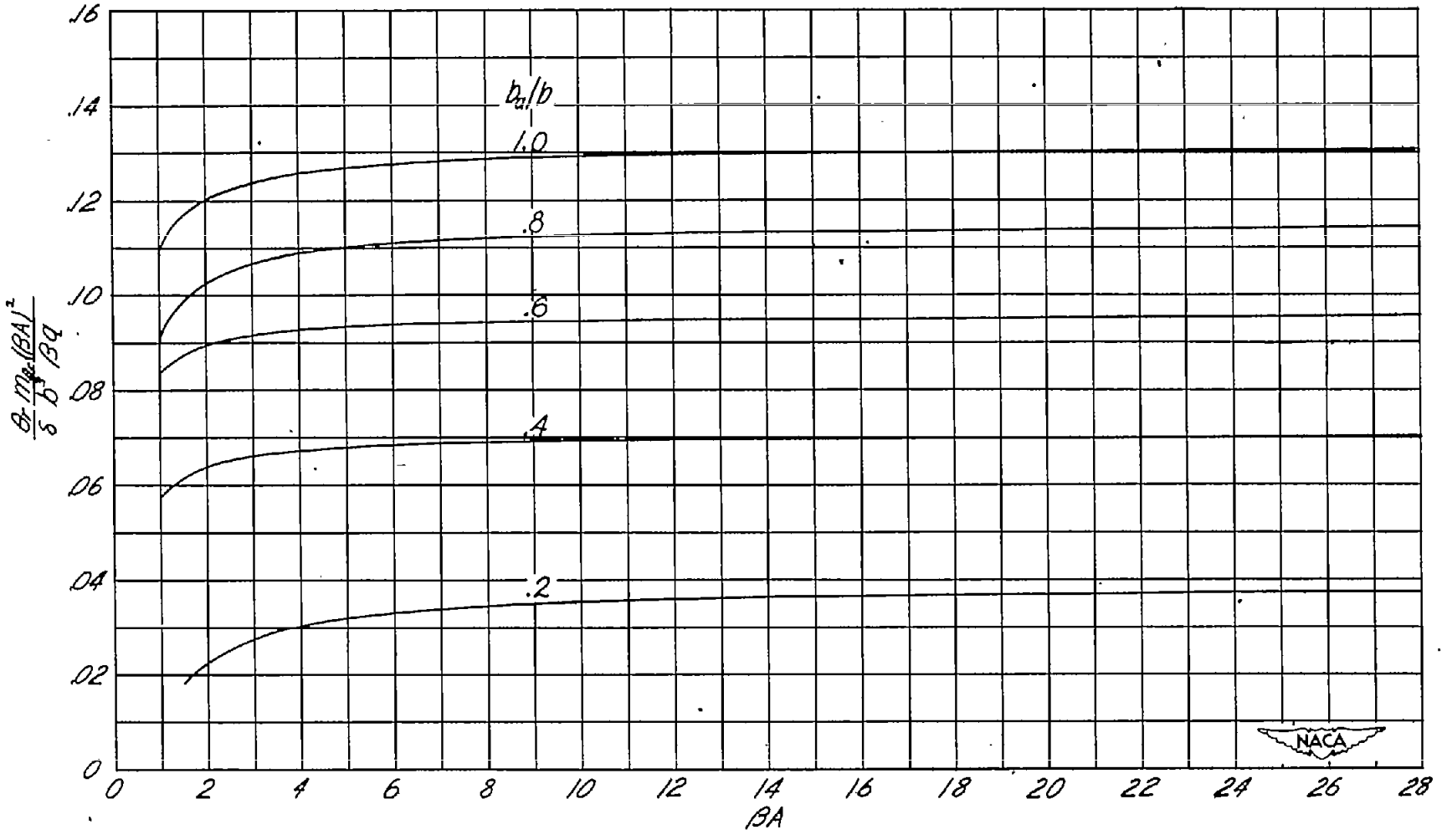


(c) $\frac{c_a}{c} = 0.3$.

Figure 11.- Concluded.

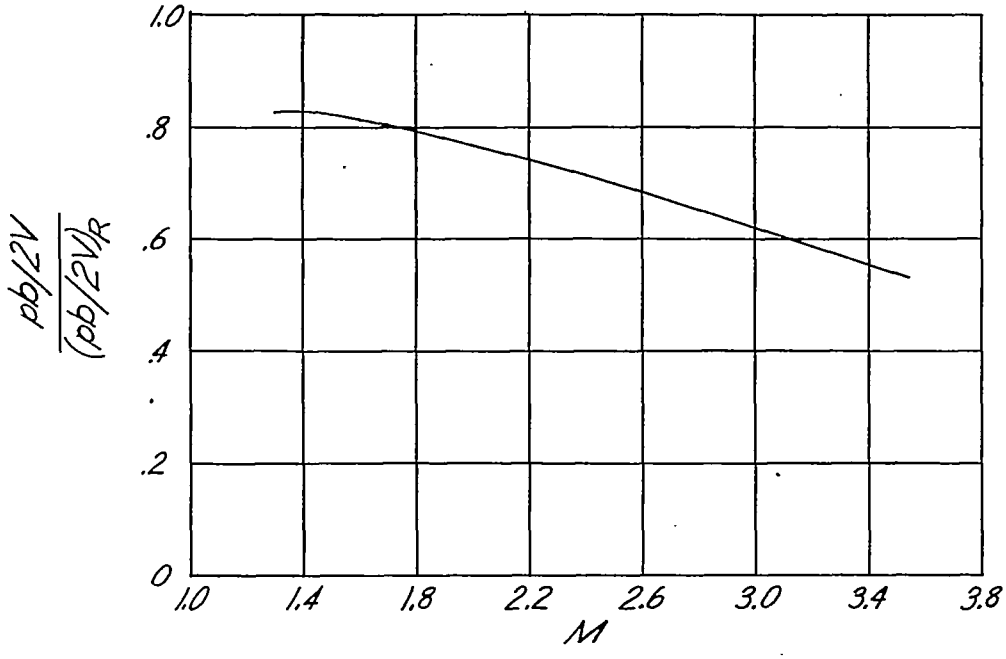


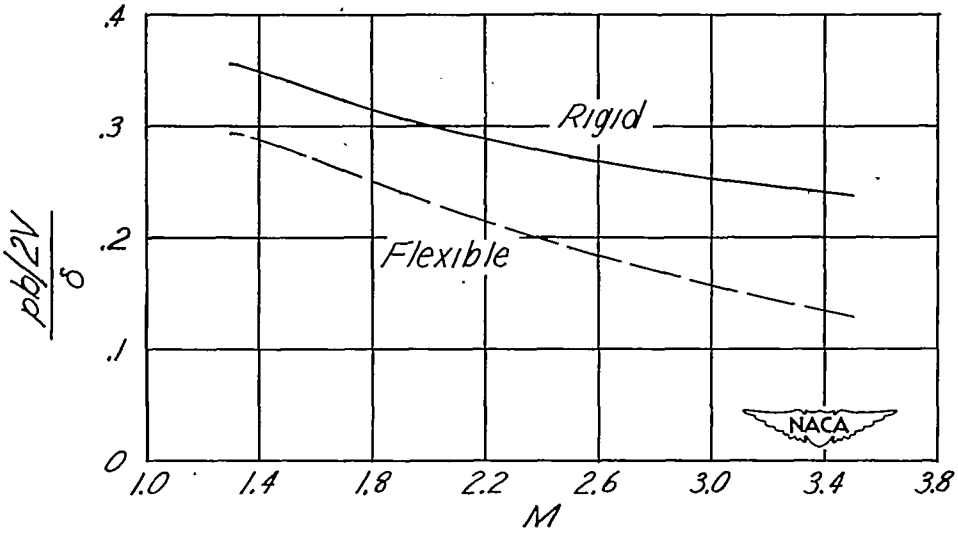


Figure 12.- Results of computations for a typical free-flight research model at sea level. A = 4; $\frac{b_a}{b}$ = 1.0; $\frac{c_a}{c}$ = 0.2; b = 2 feet; $m_{\theta_r}$ = 5000 foot-pounds per radian; and trailing-edge angle = 8°.

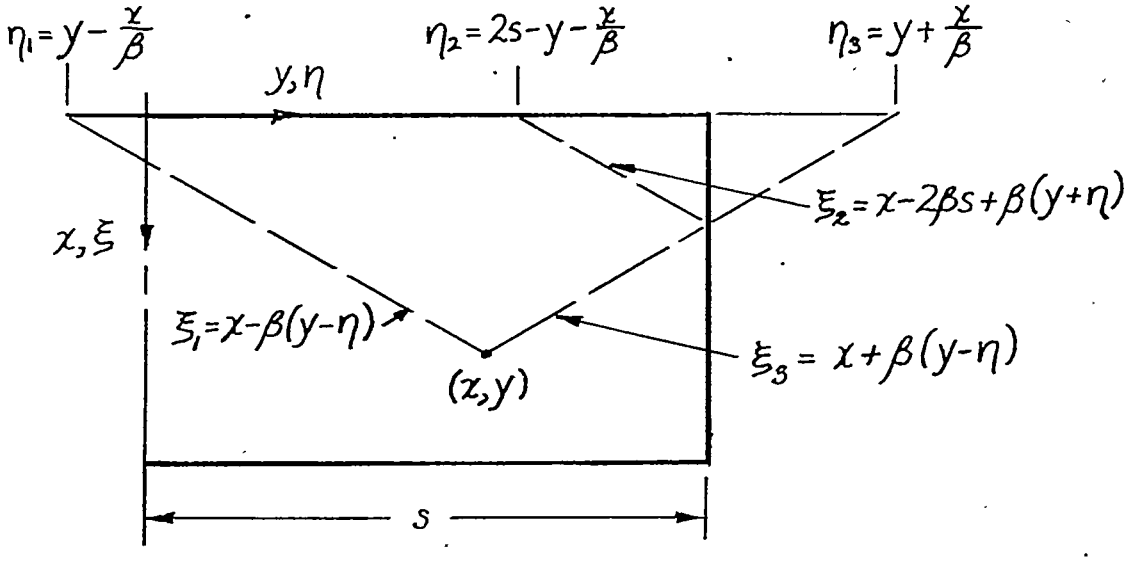


(a) Limits of integration for pressure distribution.

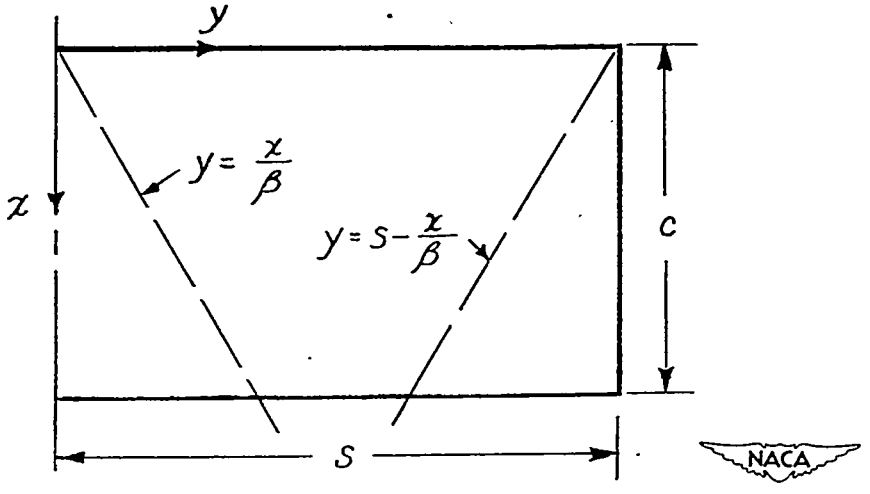


(b) Limits of integration for rolling moment.

Figure 13.- The single wing panel considered in the appendix.